

# The Effect of Stirrup Spacing on the Ultimate Load of Reinforced Concrete Beams Subjected to Pure Torsion

John Sander Nielsen

Serie R

No 180

1984

THE EFFECT OF STIRRUP SPACING ON  
THE ULTIMATE LOAD OF REINFORCED  
CONCRETE BEAMS SUBJECTED TO PURE  
TORSION

John Sander Nielsen

**The Effect of Stirrup Spacing on the Ultimate Load of Reinforced  
Concrete Beams Subjected to Pure Torsion**

Copyright © by John Sander Nielsen 1984

Tryk:

Afdelingen for Bærende Konstruktioner

Danmarks Tekniske Højskole

Lyngby

ISBN 87-87336-10-3

LIST OF CONTENTS

PREFACE .....	2
SUMMARY .....	3
NOTATIONS .....	4
1. MODEL PROPOSED BY DENIS MITCHELL, PAUL LAMPERT AND MICKAEL P. COLLINS .....	5
2. METHOD OF ANALYSES .....	8
2.1 Distribution of pressure from the concrete .....	8
2.2 Bearing capacity formula .....	12
3. DESCRIPTION OF TESTS .....	21
3.1 Object of test and description of test specimens .....	21
3.2 General remarks .....	21
3.3 Reinforcement .....	21
3.4 Concrete .....	26
3.5 Test arrangement .....	28
3.6 Measurements .....	30
3.7 Data-processing .....	33
4. COMPARISON BETWEEN EXPERIMENTAL AND THEORETICAL RESULTS ...	34
5. CONCLUSION .....	44
APPENDIX .....	48
FOTOS .....	50
MEASUREMENTS .....	59
REFERENCES .....	92

PREFACE

The purpose of this report is to clarify the effect of the stirrup spacing on the load-carrying capacity of reinforced concrete beams subjected to pure torsion. This is done both theoretically and by means of a description of 12 tests carried out at the Department of Structural Engineering of the Technical University of Denmark in the autumn of 1977. The theoretical study and the tests were carried out by the author in cooperation with Professor dr.techn. Troels Brøndum-Nielsen. The Danish Council for Scientific and Industrial Research supported the project financially, and the Department of Structural Engineering assisted in the tests.

November 1982

John Sander Nielsen

## SUMMARY

There appear to be very few reports on the effect of stirrup spacing on the load-carrying capacity of concrete beams subjected to torsion (or, in general, on the effect of the design of the reinforcement). Here, only one report, by Denis Mitchell, Paul Lampert and Michael P. Collins [1], will be discussed in detail (in section 1).

In section 2, a theory is advanced which deals with the problems on different assumptions than those applied in [1], while section 3 contains a description of the tests carried out. Finally, in section 4 the theory is compared with the results of the tests, and section 5 contains a conclusion.

## SUMMARY in Danish (Dansk Resumé)

Hvad der foreligger af rapporter omhandlende bøjleafstandens (eller i det hele taget armeringsudformningens) betydning for vridningspåvirkede betonbjælkens bæreevne er yderst sparsomt. Her skal kun én rapport af Denis Mitchell, Paul Lampert og Michael P. Collins, [1], omtales nærmere (afsnit 1).

I afsnit 2 søges opstillet en teori, der, ud fra andre forudsætninger end de i [1] gjorde, belyser problemerne, medens afsnit 3 er en beskrivelse af de udførte forsøg. Endelig er teori og forsøg søgt sammenlignet i afsnit 4, og der afsluttes i afsnit 5 med en konklusion.

NOTATION

- $T$  = Torsional moment
- $T_n$  = Torsional strength (Lattice analogy method)
- $P_a$  = The yield force in a corner reinforcing bar
- $P_{ah}$  = The horizontal component of  $P_a$
- $P_{av}$  = The vertical component of  $P_a$
- $P_b$  = The yield force in a stirrup
- $p(x)$  = Load per unit length of the corner reinforcement
- $n_{xa}$  = The force in the reinforcement per unit length  
(in the longitudinal direction)
- $n_{ya}$  = The force in the reinforcement per unit length  
(in the stirrup direction)
- $\left. \begin{array}{l} a \\ b \end{array} \right\}$  = The side lengths of the rectangle formed by the  
longitudinal reinforcement.
- $\Sigma A_e$  = Area of the total reinforcement in the axial  
direction
- $A_{co}$  = Area of the weakest corner reinforcing bar
- $s$  = Stirrup spacing
- $d_{co}$  = Diameter of the weakest corner reinforcing bar
- $u$  = Circumference of the rectangle formed by the  
corner reinforcing bar
- $n$  = The ratio between the total force in the reinforce-  
ment in the longitudinal direction and the sum of  
the force in the corner reinforcement

1. MODEL PROPOSED BY DENIS MITCHELL, PAUL LAMPERT  
AND MICHAEL P. COLLINS [1]

In [1], only beams of rectangular cross-section, reinforced with longitudinal reinforcement lying along the sides of the cross-section and with closed stirrups at an angle of  $90^\circ$  with the axis of the beam, are considered.

The statical mode of operation of the beams is assumed to be the same as that of a lattice system with N-lattice, in which the reinforcement consists of flanges and verticals, while the concrete acts in the same way as the diagonals (lattice analogy method - see, for example, [2]).

The problem of finding a maximum permissible stirrup spacing is approached by regarding the corner reinforcing bars as continuous beams supported by the stirrups. The materials are taken to be plastic, and the following assumptions are applied:

1. Same reinforcing force in the direction of the stirrups and the axial direction per unit length (of axial direction and of direction of stirrups).
2. The load on the beams (corner reinforcement) is the diagonal pressure exerted by the concrete.
3. The pressure is assumed to be uniformly distributed, although regarding the loads it is stated that these are of a discrete nature and that they occur randomly due to the unpredictable crack location. The result of this is a rigid block type of loading that can substantially reduce the moment. It is further assumed that it is possible for shear force to be transmitted along the tensile cracks. Both these factors are taken into account by putting the maximum moments (in the corner reinforcing bars) at  $\beta$  times the moment in the case of uniformly distributed load.



4. In the calculation of the maximum permissible moment, this is assumed to be equal to  $\alpha$  times the plastic bending moment (without normal force) - where  $\alpha$  denotes the incremental effect of the surrounding concrete on the resistance moment.

Equating the permissible with the actual moment, and comparing this with the available test results, we get:

$$\frac{\Sigma A_e}{A_{CO}} \cdot \frac{s}{d_{CO}} \cdot \frac{s}{u} \leq \sqrt{2} \frac{\alpha}{\beta} = 25$$

where

$\Sigma A_e$  = area of the total reinforcement in the axial direction

$A_{CO}$  = area of the weakest corner reinforcing bar

$s$  = stirrup spacing

$d_{CO}$  = diameter of the weakest corner reinforcing bar

$u$  = circumference of the rectangle formed by the corner reinforcing bars.

By plotting the test results as a function of  $s/d_{CO}$ , it is, in fact, shown that yielding of the reinforcement occurs when

$$s/d_{CO} \leq 16$$

From the test material it is further found that

$s/u$  should be chosen smaller than or equal to  $1/8$  and the authors advise choosing

$$s \leq 0.3 \text{ m}$$

However, the determination of  $\frac{\alpha}{\beta}$  on the basis of the tests reported cannot be said to be reasonably accurate, and on the face of it, the value of  $\frac{\alpha}{\beta}$  ( $\frac{\alpha}{\beta} = 17.7$ ) appears high. The latter comment applies particularly in the case of normally reinforced beams, where the plastic moment of resistance of the corner reinforcing bars approaches zero (on account of the normal force) when the torsional moment approaches the ultimate value.

Finally, it must be mentioned that the ratio  $\frac{\alpha}{\beta}$  need not necessarily be a constant that is independent of such parameters as the diameter of the corner bars, the stiffness (strength) of the concrete and the design of the reinforcement.

## 2. METHOD OF ANALYSIS

Here, the problem is approached on the basis of other assumptions than those made in [1] with regard to the mode of operation of the corner reinforcing bars, but with the same assumptions regarding the construction and mode of operation of the beam.

### 2.1 Distribution of pressure from the concrete

Unlike the case in Section 1, the longitudinal reinforcement is here regarded as being flexurally weak, i.e. it is assumed to have a moment of resistance  $\approx 0$ . The closer the load in the beam to the ultimate load, the better this assumption will be fulfilled, and for normally reinforced beams, it will be satisfied when the ultimate load is reached.

We will now perform the idealization indicated in fig. 1.

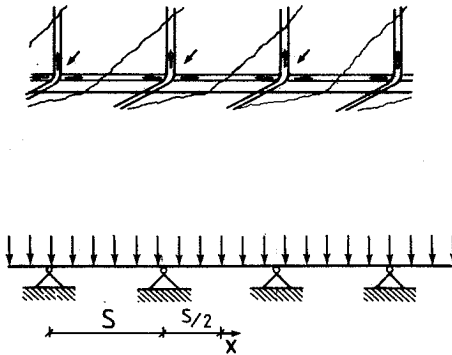


Fig. 1.

Here, the reinforcing bar in the corner is regarded as a flexurally weak, continuous cable, supported at each stirrup and subjected to a linear load  $p(x)$ . Two limit cases can be imagined for the distribution of  $p(x)$ :

- a) uniformly distributed load
- b) distribution corresponding to the concrete being a homogeneous, perfectly plastic material.

a) uniformly distributed load:

$$p(x) = \text{constant} = p$$

The deflection curve will be a parabola (see [5] with the equation:

$$y = \frac{4f}{s^2} x^2$$

$$\text{for } -\frac{1}{2}s \leq x \leq \frac{1}{2}s ;$$

where  $f$  is the camber of the parabola and the coordinate system is inserted as shown in fig. 2.

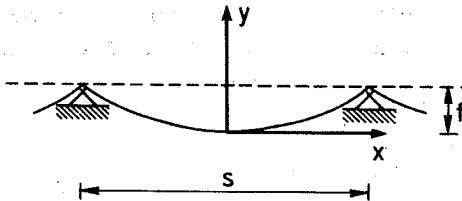


Fig. 2.

b) elastic model:

$$p(x) = -ky$$

The differential equation for the problem (see [5]) is:

$$\frac{d^2y}{dx^2} = -\frac{k}{N}p(x)$$

where  $N$  is a constant equal to the horizontal force, and  $k$  is a constant dependent on the modulus of elasticity of the concrete.

Inserting  $p(x)$ , we obtain:

$$\frac{d^2y}{dx^2} - \frac{k}{N}y = 0$$

Solution:

$$y = C_1 \cosh \lambda x + C_2 \sinh \lambda x$$

$$\lambda = \sqrt{\frac{k}{N}}$$

$C_2$  is determined as zero (for reasons of symmetry)

$C_1$  is determined by integration of  $k \cdot y$  over the length  $s$  - this integral must be equal to the component of the stirrup forces after the bisector of the corner.

$$C_1 = \frac{\sqrt{2} \cdot P_b \cdot \lambda}{2k \sinh \lambda \frac{s}{2}}$$

where

$P_b$  = the stirrup force.

Inserting  $C_1$ , we obtain:

$$y = \frac{1}{\sqrt{2} \cdot \sqrt{k} \cdot N} P_b \frac{\cosh \lambda \cdot x}{\sinh \lambda \cdot \frac{S}{2}}$$

$$|p(x)| = \frac{1}{\sqrt{2}} \cdot P_b \lambda \frac{\cosh \lambda \cdot x}{\sinh \lambda \cdot \frac{S}{2}}$$

where the coordinate system is located as indicated in fig. 3.

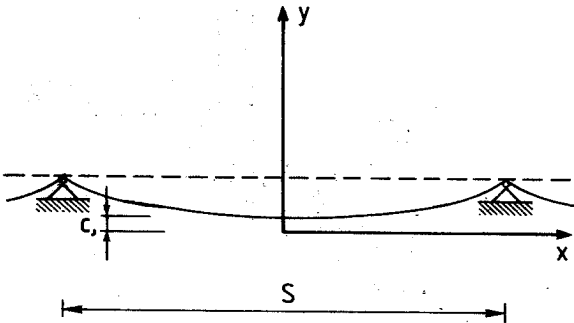


Fig. 3.

It is reasonable to suppose that the distribution calculated under point b) will be the first to occur, and that an equalization will take place as the cracking of the beam becomes more pronounced and as  $p(x)$  under the stirrups exceeds the limit below which the concrete can be assumed to be perfectly elastic. Numerical values have not been inserted because several of the parameters cannot be estimated with reasonable accuracy.

## 2.2 Bearing capacity formula

In order to arrive at a viable expression for the torsional strength of the beam as a function of the stirrup spacing, it is not, however, necessary to know the true distribution of the concrete pressure along the reinforcing bars in the corners.

Let us consider a corner member as shown in fig. 4.

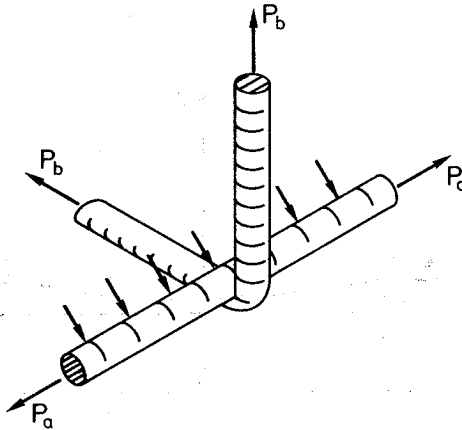


Fig. 4.

Neglecting the part of the concrete stresses that may possibly be transmitted to the stirrup through direct contact, we obtain the following by projection on the plane formed by the bisector of the corner under consideration:

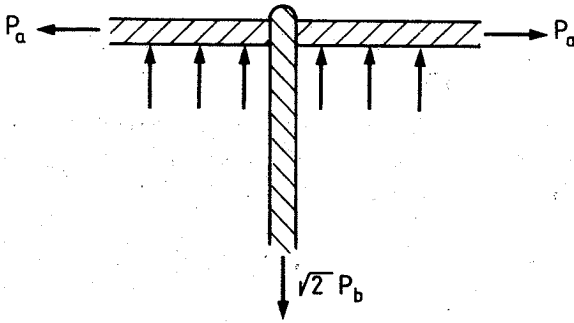


Fig. 5.

As the axial reinforcement is assumed to have no flexural strength, it is necessary, in order to create equilibrium, for the axial reinforcing bar to bend outwards, as shown in fig. 6.

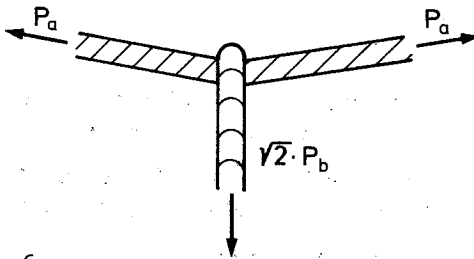


Fig. 6.

with the following force diagram:

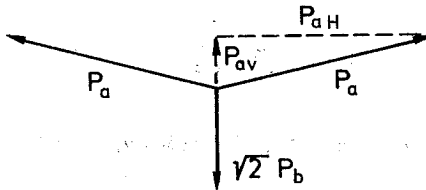


Fig. 7.



From vertical projection, we obtain from fig. 7:

$$P_{av} = \frac{1}{\sqrt{2}} P_b$$

Of  $P_a$ , only the component  $P_{aH}$  remains to resist the torsional moment. The magnitude of  $P_{aH}$  is found from the following expression:

$$P_{aH} = \sqrt{P_a^2 - P_{av}^2} = \sqrt{P_a^2 - \frac{1}{2}P_b^2}$$

If we calculate the carrying capacity by means of the lattice analogy method (see, for example, [2]), we obtain the following for underreinforced beams with only one longitudinal bar in each corner:

$$T = 2 \cdot a \cdot b \cdot \sqrt{\frac{P_b}{s} \cdot \frac{P_{aH}}{\frac{a+b}{2}}} \quad (I)$$

where

$a$  = the length of one side of the rectangle formed by the axial reinforcement,

$b$  = the length of the other side of the rectangle formed by the axial reinforcement,

$s$  = the stirrup spacing.

The expression normally used for the torsional strength  $T_n$  is (see, for example, [2]):

$$T_n = 2 \cdot a \cdot b \cdot \sqrt{\frac{P_b}{s} \cdot \frac{P_a}{\frac{a+b}{2}}} \quad (II)$$

Inserting  $T_n$  and  $P_{aH}$  in the expression for  $T$ , we obtain:

$$T = T_n \cdot \sqrt[4]{1 - \frac{1}{2} \left(\frac{P_b}{P_a}\right)^2} \quad (III)$$

Fig. 8 shows the expression (the reduction factor):

$$f\left(\frac{P_b}{P_a}\right) = \frac{T}{T_n} = \sqrt[4]{1 - \frac{1}{2}\left(\frac{P_b}{P_a}\right)^2}$$

depicted as a function of  $\frac{P_b}{P_a}$ .

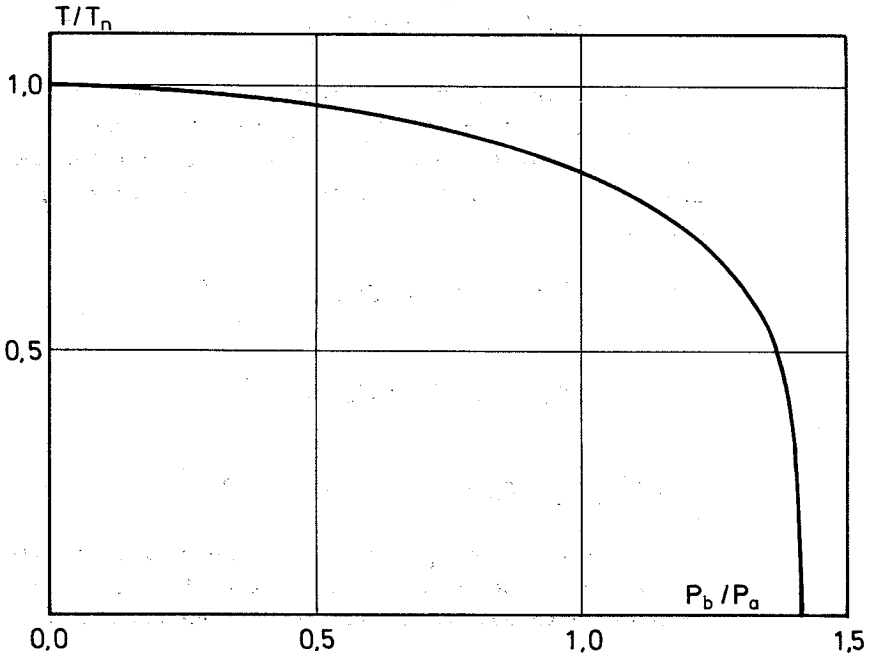


Fig. 8.

In accordance with the expression:

$$\begin{aligned} T &= 2ab \cdot \sqrt{\frac{P_b}{s} \cdot \frac{P_a H}{a+b}} \\ &= 2ab \cdot \sqrt{\frac{P_b}{s} \cdot \frac{2}{a+b} \sqrt{P_a^2 - \frac{1}{2} P_b^2}} \\ &= 2ab \cdot \sqrt{\frac{2}{s(a+b)} \sqrt{P_a^2 P_b^2 - \frac{1}{2} P_b^4}} \quad \text{(IV)} \end{aligned}$$

T increases throughout with increasing  $P_a$ , while  $T = 0$  for  $P_b = 0$  and for  $P_b = P_a \cdot \sqrt{2}$ . T assumes positive values for  $0 \leq P_b \leq P_a \cdot \sqrt{2}$ , and must therefore have a maximum for a value of  $P_b$  between these bounds.

T is maximum when  $P_a^2 P_b^2 - \frac{1}{2} P_b^4$  has a maximum.

$$\frac{\partial}{\partial P_a} (P_a^2 P_b^2 - \frac{1}{2} P_b^4) = 2 P_a P_b^2 - \frac{1}{2} \cdot 4 P_b^3$$

$$2 P_a^2 P_b - \frac{1}{2} \cdot 4 P_b^3 = 0 \quad \text{for } P_b = P_a$$

In other words, for  $P_b > P_a$  we get the maximum torsional strength when the force in one stirrup leg does not reach yield value, but is limited to the value  $P_a$ .

In such case, for  $P_b \geq P_a$ , we obtain from IV :

$$\begin{aligned}
 T &= 2ab \sqrt{\frac{2}{s(a+b)}} \sqrt{P_a^4 - \frac{1}{2} P_a^4} \\
 &= 2ab \sqrt{\frac{2}{s(a+b)}} P_a^2 \cdot \sqrt{\frac{1}{2}} \\
 &= 2ab \sqrt{\frac{2}{s(a+b)}} P_a \frac{P_a}{P_b} \cdot P_b \cdot \sqrt{\frac{1}{2}} \\
 &= T_n \sqrt[4]{\frac{1}{2} \left(\frac{P_a}{P_b}\right)^2} \tag{V}
 \end{aligned}$$

The torsional strength can therefore be determined as

$$T = T_n \cdot f\left(\frac{P_b}{P_a}\right)$$

where

$T_n$  = the carrying capacity calculated on the basis of the lattice analogy method,

$$f\left(\frac{P_b}{P_a}\right) = \begin{cases} \sqrt[4]{1 - \frac{1}{2} \left(\frac{P_b}{P_a}\right)^2} & \text{for } P_b \leq P_a \\ \sqrt[4]{\frac{1}{2} \left(\frac{P_a}{P_b}\right)^2} & \text{for } P_b \geq P_a \end{cases}$$

The function  $f$  is depicted in fig. 9.

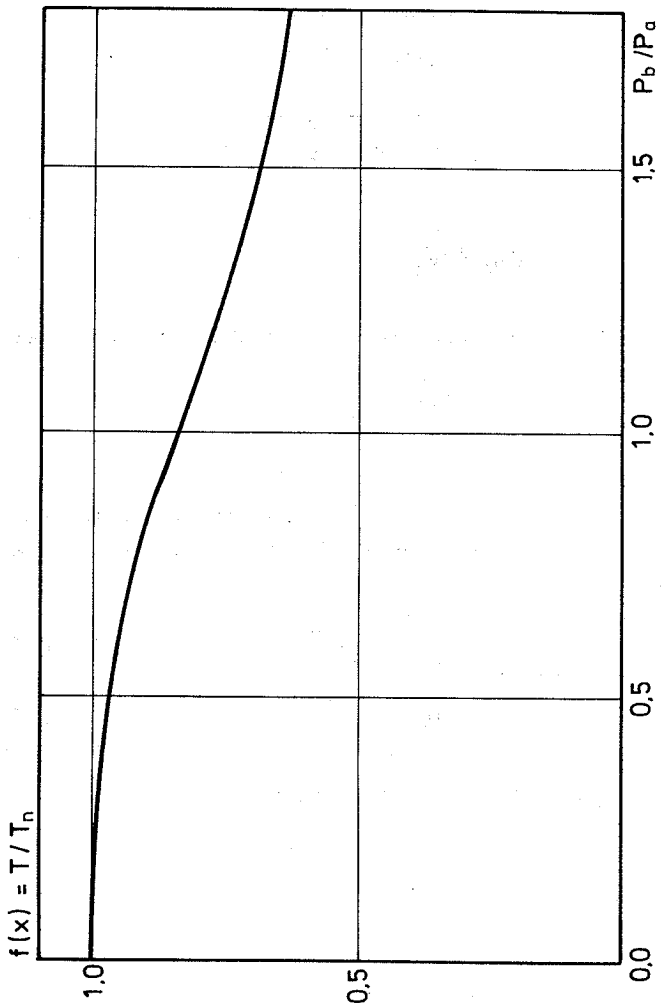


Fig. 9.

Beams with more than four longitudinal reinforcing bars are calculated in a similar manner. It is assumed here that failure occurs in the axial reinforcement near the corners.

Denoting as  $n$  the ratio between the total force in the longitudinal reinforcement and the force in the corner reinforcement, we can change equation I to:

$$T = 2 \cdot a \cdot b \cdot \sqrt{\frac{P_b}{s} \cdot \frac{P_{aH} + (n-1)P_a}{\frac{a+b}{2}}}$$

and equation II to:

$$T_n = 2 \cdot a \cdot b \cdot \sqrt{\frac{P_b}{s} \cdot \frac{P_a}{\frac{a+b}{2}} \cdot n}$$

whereby (without altering the expression for  $P_{aH}$ ), equation III becomes:

$$T = T_n \cdot \sqrt{\frac{(n-1) + \sqrt{1 - \frac{1}{2} \left(\frac{P_b}{P_a}\right)^2}}{n}}$$

Defining  $\gamma$  as the value of the ratio  $\frac{P_b}{P_a}$  that maximizes the expression:

$$T = 2 \cdot a \cdot b \cdot \sqrt{\frac{P_b}{s} \cdot \frac{P_{aH} + (n-1)P_a}{\frac{a+b}{2}}}$$

we obtain, by differentiating with respect to  $P_b$ :

$$\gamma = \sqrt{1 - \frac{1}{4}(n-1)^2 + \frac{1}{4}(n-1) \sqrt{(n-1)^2 + 8}}$$

By inserting this expression in

$$T = 2ab \sqrt{\frac{P_b}{s} \cdot \frac{P_{aH} + (n-1)P_a}{\frac{a+b}{2}}}$$

we obtain, in analogy with equation V:

$$T = T_n \cdot \sqrt{\frac{\gamma(n-1) + \sqrt{\gamma^2 - \frac{1}{2}\gamma^4}}{n} \frac{P_a}{P_b}}$$

The torsional strength can therefore be determined for  $n \geq 1$  by means of the following expression:

$$T = T_n \cdot f\left(\frac{P_b}{P_a}\right)$$

where  $T_n$  = the carrying capacity calculated on the basis of the lattice analogy method

$$= 2 \cdot a \cdot b \cdot \sqrt{\frac{P_b}{s} \cdot \frac{n \cdot P_a}{(a+b)^2}}$$

$$f\left(\frac{P_b}{P_a}\right) = \begin{cases} \sqrt{\frac{(n-1) + \sqrt{1 - \frac{1}{2}\left(\frac{P_b}{P_a}\right)^2}}{n}} & \text{for } P_b \leq \gamma P_a \\ \sqrt{\frac{\gamma(n-1) + \sqrt{\gamma^2 - \frac{1}{2}\gamma^4}}{n}} \left(\frac{P_a}{P_b}\right) & \text{for } P_b \geq \gamma P_a \end{cases}$$

where  $1 \leq \gamma < \sqrt{2}$  is determined from:

$$\gamma = \sqrt{1 - \frac{1}{4}(n-1)^2 + \frac{1}{4}(n-1) \sqrt{(n-1)^2 + 8}}$$

### 3. DESCRIPTION OF TESTS

#### 3.1 Object of test and description of test specimens

In order to evaluate the theory formulated in section 2 and to investigate the mode of failure in the case of big stirrup spacing, a series of tests was carried out on concrete beams subjected to torsion. The series comprised 12 beams, two of which were partially pre-stressed. The arrangement of the reinforcement is shown in fig. 10 and fig. 11. The tests were performed 14 days after casting of the beams (4 days' curing under wet sacks and 10 days in the testing laboratory at about 21°C and 50%RH).

#### 3.2 General remarks

In the following, a complete description is not given of the test apparatus, the material properties of the components, etc., because these were precisely as described for the test series in [3], to which readers are referred for additional information.

#### 3.3 Reinforcement

The reinforcement used was round bars and Danish deformed bars. The dimensions 7 and 8 mm were normalized at 860°-880°C, followed by air-cooling. One test bar of each length was extracted and tested, but as the deviations in the test results within each dimension were less than 1%, only the average values of the yield stress and ultimate strength are given (see table 1). Figure 12 shows a typical stress-strain curve for the types of steel used.



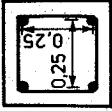
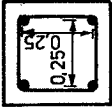
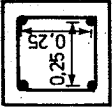
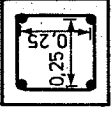
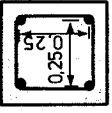
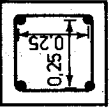
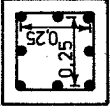
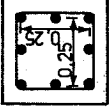
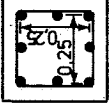
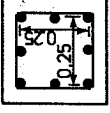
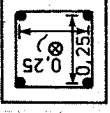
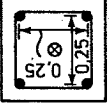
Beam No.	I-1	I-2	I-3	I-4	I-5	I-6
Cross Sections 0,3 x 0,3 m						
Long steel	KS 42 S d = 10 mm	KS 42 S d = 10 mm	KS 42 S d = 10 mm	KS 42 S d = 10 mm	KS 56 S d = 10 mm	KS 56 S d = 10 mm
Stirrups	R 37 d = 7 mm s = 81 mm	KS 42 S d = 8 mm s = 131 mm	KS 42 S d = 10 mm s = 250 mm	KS 42 S d = 12 mm s = 350 mm	KS 56 S d = 10 mm s = 250 mm	KS 56 S d = 12 mm s = 376 mm

Fig. 10.

Beam No.	III-1	III-2	III-3	III-4	III-5	III-6
Cross Sections 0,3 x 0,3 m						
long steel	KS 42 S d = 10 mm	KS 42 S d = 10 mm	KS 42 S d = 10 mm	KS 42 S d = 10 mm	KS 42 S d = 10 mm	KS 42 S d = 10 mm
Stirrups	KS 42 S d = 8 mm s = $\frac{131}{2}$ mm	KS 42 S d = 10 mm s = 125 mm	KS 42 S d = 12 mm s = 175 mm	KS 90 S d = 12 mm s = 339 mm	KS 42 S d = 10 mm s = 125 mm	KS 42 S d = 12 mm s = 175 mm

\* and a  $\frac{1}{4}$ " prestressed tendon placed in the centre of the cross section.

Fig. 11.

Kvalitet	Dimension mm	$P_f$ KN	$\epsilon_f$	$P_{brud}$ KN
R 37	7	12.50	0.00140	18.0
KS 42 S	8	20.40	0.00200	31.1
	10	38.57	0.00226	50.9
	12	53.96	0.00202	73.1
KS 56 S	10	49.75	0.0032	63.2
	12	74.40	0.0032	97.5
KS 90 S	12	104.70	0.00455	113.8

Table 1. Steel strengths

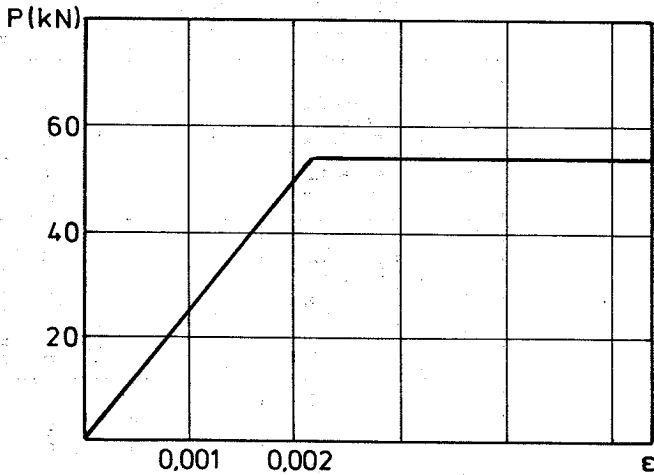


Fig. 12

In beams II-5 and II-6, a half-inch prestressed tendon (English normal relaxation steel) was also used.

The ultimate load for the cables was 175 kN, and the cables were prestressed to about 140 kN (about 80%). The curve for the loss of prestress on account of relaxation has been taken from tests carried out at the Structural Research Laboratory of the Technical University of Denmark in 1975 and is published in [6]. The steel tested here was of the same quality as the steel used for the tests, except that the tendon diameter was 0.6". The prestress was 80%.

### 3.4 Concrete

Three types of concrete were used, with the following compositions, where the cement used was Portland rapid.

For beams I-1, I-2, I-3, I-4 and I-5:

water	164 kg/m <sup>3</sup>
cement	205 kg/m <sup>3</sup>
fine agg.	846 kg/m <sup>3</sup>
coarse agg.	1119 kg/m <sup>3</sup>

For beam I-6:

water	200 kg/m <sup>3</sup>
cement	128 kg/m <sup>3</sup>
fine agg.	1305 kg/m <sup>3</sup>
coarse agg.	945 kg/m <sup>3</sup>

For beams II-1, II-2, II-3, II-4, II-5 and II-6:

water	167 kg/m <sup>3</sup>
cement	300 kg/m <sup>3</sup>
fine agg.	717 kg/m <sup>3</sup>
coarse agg.	1167 kg/m <sup>3</sup>

For each beam, 6 cylinders were cast for compression testing and 6 cylinders for splitting tests.

The strength values measured and their standard deviations are shown in table 2.

Table 2. Concrete strengths

Beam No.	Compression strength MPa		Splitting strength MPa	
	mean value	devia-tion	Mean value	devia-tion
I-1	20.99	0.830	2.662	0.101
I-2	20.52	0.653	2.149	0.356
I-3	22.23	0.643	2.780	0.128
I-4	21.50	1.442	2.343	0.249
I-5	22.08	0.580	2.350	0.413
III-1	38.68	1.345	3.269	0.145
III-2	37.88	1.260	3.326	0.165
III-3	38.16	1.150	3.579	0.213
III-4	39.62	1.112	3.204	0.284
III-5	44.16	0.643	3.596	0.159
III-6	44.80	2.093	3.239	0.239

### 3.5 Test arrangement

Fig. 15 shows the statical mode of operation of the test arrangement, while fig. 16 shows a photo of the apparatus.

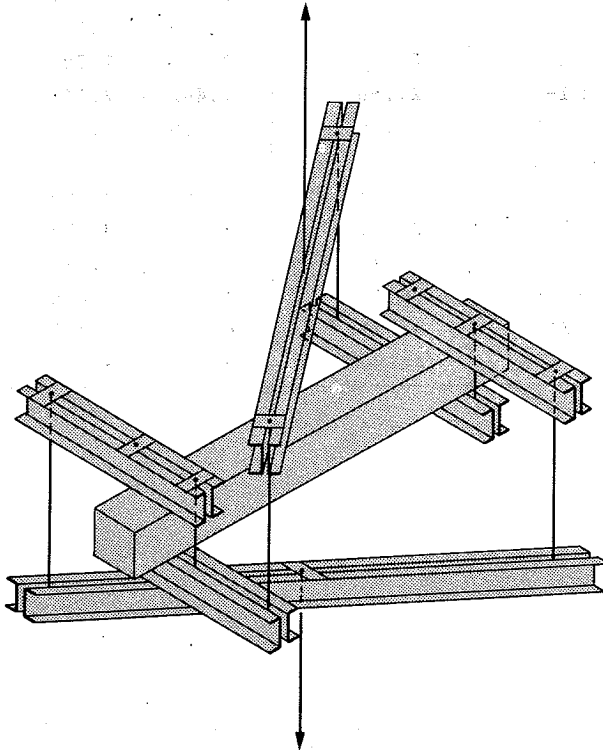


Fig. 15

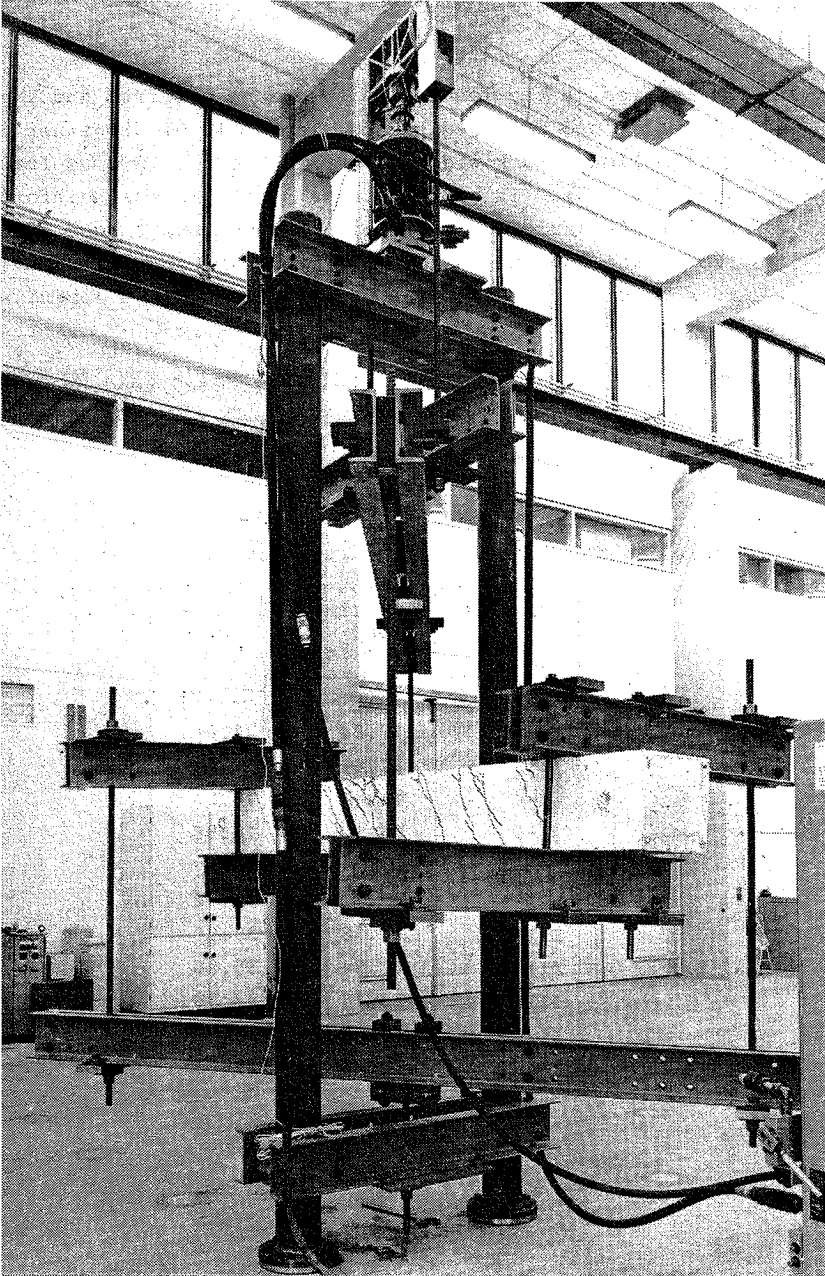


Fig. 16.



### 3.6 Measurements

In the tests, the load at which cracks occurred and the ultimate load were registered (see table 3), together with maximum crack widths occurring at the various loads (see fig. 17). In addition, the strain in the reinforcement was measured by means of strain gauges placed on two of the longitudinal reinforcing bars and on the stirrups on either side of the middle stirrup (see appendix).

The strain measurements in the prestressed tendons were taken by means of strain gauges placed as shown in fig. 18.

Table 3. Cracking load and ultimate load

Beam No.	Cracking load kNm	Ultimate load kNm
I-1	18.91	22.22
I-2	17.84	21.04
I-3	17.84	17.84
I-4	17.84	17.84
I-5	15.72	18.86
III-1	25.31	41.72
III-2	23.18	35.96
III-3	22.54	35.96
III-4	23.18	23.18
III-5	30.64	41.29
III-6	27.44	37.03

CRACK WIDTH

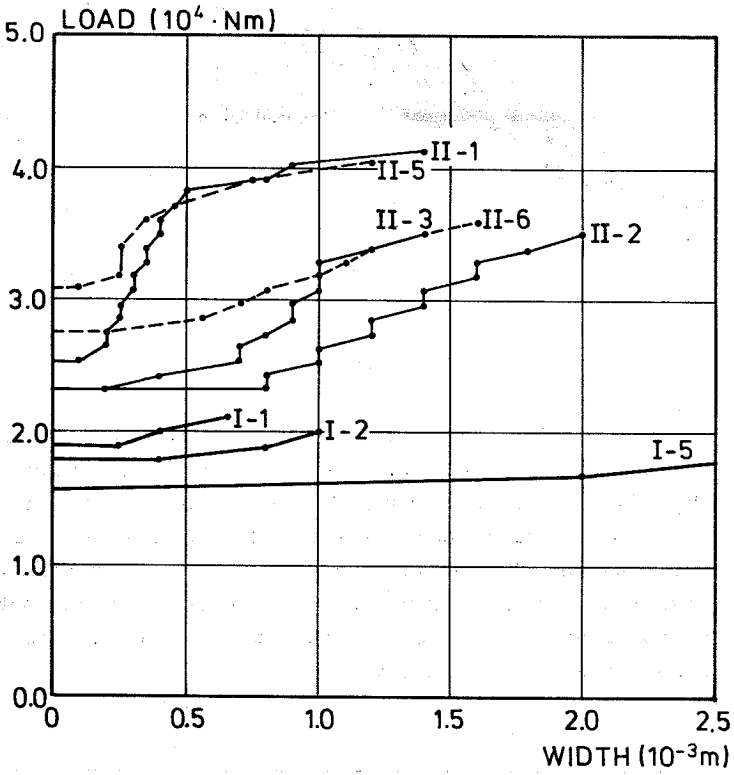


Fig. 17

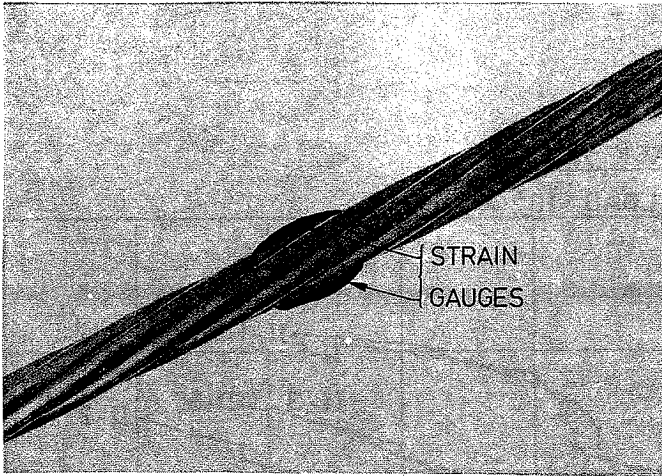


Fig. 18.

On account of the inclination of the wires, the strain measure is not equal to the elongation of the tendon. Therefore, on a test bar, the relationship between the strain measure used here and the force in the tendon was measured. In addition, the rotation of the beam was measured with angular potentiometers glued to the bottom of the beam (see appendix). The positions of the potentiometers are shown in fig. 19.

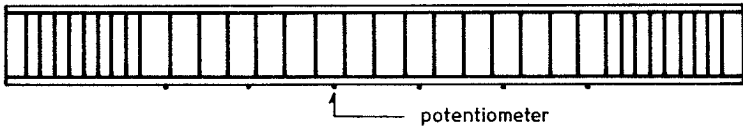


Fig. 19.

### 3.7 Data-processing

All the test results were put out on punch tape, converted to punch cards and then processed by means of a computer program developed for the purpose. The results from the material tests were coded on punch cards and also included in the program.

The following were computed for each loading step:

- Rotations
- Mean rotation per unit of length
- Strain in reinforcement
- Mean strain in reinforcement
- Differential strain
- Forces in reinforcement

In addition, the material constants and the standard deviations on these were computed.

The following curves were plotted (see appendix):

- Loading history
- Rotation
- Stress-strain curve for the beam
- Strain in the reinforcement (mean and differential)
- Forces in the reinforcement.

4. COMPARISON BETWEEN EXPERIMENTAL AND THEORETICAL RESULTS

The comparison between test and theory is mainly concentrated on the following two points:

1. comparison between the modes of behaviour assumed in sections 1 and 2 and those observed in the tests;
2. comparison between the calculated and the measured values of the ultimate strengths of the beams.

Re. 1.

The theory of D. Mitchell, P. Lampert and M. P. Collins, described in section 1, operates with a deflection pattern for the corner reinforcing bars as shown in fig. 20, whereas the theory in section 2 assumes that the deflection pattern is a collection of smooth curves composed of parabolic and hyperbolic cosine curves.

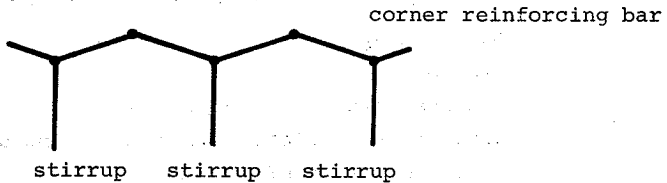


Fig. 20.

If we consider a beam in which the reinforcement has reached its yield stress (normally reinforced), the deflection patterns for the corner reinforcing bars at the ultimate load will not change during unloading, and we can therefore obtain an impression of the mechanism chosen by the reinforcing bar by cutting away the cover.



Fig. 21.

The photo shown in fig. 21 is taken from P. Lampert, P. Lüchinger and B. Thürlimann: Torsionsversuche an Stahl- und Spannbetonbalken [4] and shows the beam  $T_9$ , which contains not only the reinforcement shown, but also a prestressed tendon in the middle of the cross-section. It will be seen that the deflection pattern is a collection of parabolic curves with points of discontinuity under the stirrups, and there is nothing to indicate the formation of a plastic hinge halfway between 2 stirrups.

Fig. 22 and fig. 23 are photos of corner reinforcing bars cut out of beams II-5 and II-6, and the same tendency can be noted here.

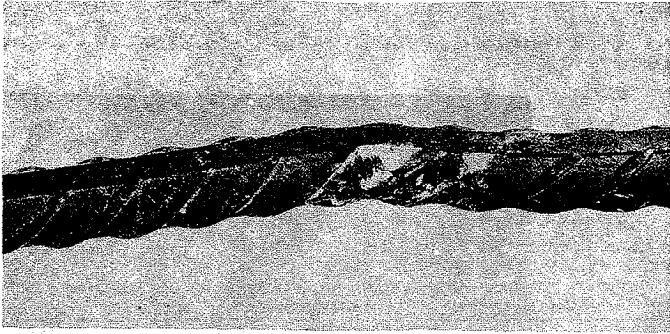


Fig. 22.

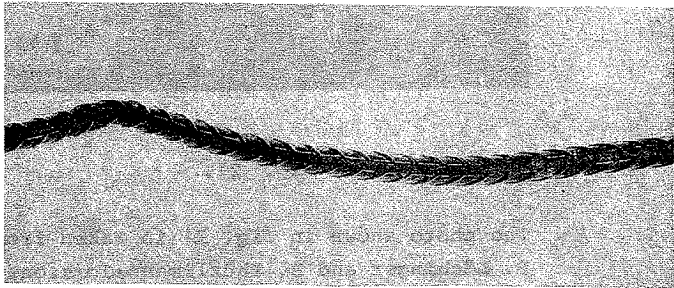


Fig. 23.

In addition, it is noted in fig. 23 that the two curves meet rather sharply at the point of discontinuity, which might indicate that the assumption made in section 2.2 - that no compressive stresses in the concrete are transmitted directly to the stirrup through contact pressure - is a reasonable one.

With regard to the failure mechanism of the beam, it is noted that no yielding of the reinforcement took place at stirrup spacings greater than the distance between the longitudinal bars in the corners. A failure mechanism occurred that was

analogous to that occurring for unreinforced beams - flexural failure about an axis parallel with the beam axis and located on one side (see fig. 24).

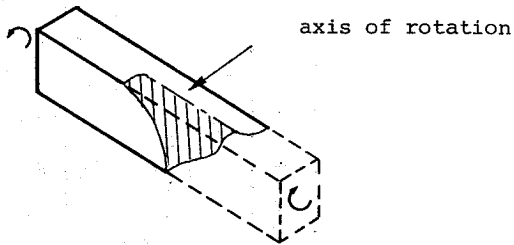


Fig. 24.

This failure mechanism does not activate any of the stirrups of the longitudinal bars, and if the ultimate load is greater than the cracking load, it must presumably be due solely to dowel action.

Re. 2.

In addition to the authors' own tests, described in section 3, the comparison between test and theory will also take account of 6 tests carried out by D. Mitchell, P. Lampert and M. P. Collins, described in [1].

Fig. 25 shows the test specifications, and table 4 shows all theoretical and experimental bearing capacities.



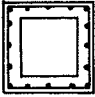

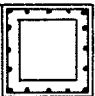
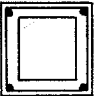


PROBLEM	STIRRUP SPACING							
	C0	C1	C2	C6	C7	C8		
BEAM NO.								
CROSS SECTIONS 17" X 17" HOLLOW								
LONG. STEEL	16 #3	16 #3	16 #3	4 #5	16 #3	16 #2		
STIRRUPS	3#3 @ 11.7	2#3 @ 7.8	1#3 @ 3.9	3#3 @ 11.7	3#3 @ 11.7	1#3 @ 6.5		

Fig. 25.

Table 4.

Beam No. [ ]	T <sub>exp</sub> i.k.	T <sub>n</sub> i.k.	T <sub>exp</sub>	T <sub>theory</sub> i.k.	T <sub>exp</sub>
			T <sub>n</sub>		T <sub>theory</sub>
C 0	441	584	0.76	356	1.24
C 1	522	594	0.88	443	1.18
C 2	590	594	0.99	575	1.03
C 6	466	546	0.85	491	0.95
C 7 <sup>+</sup>	450	594	0.76	465	0.97
C 8	294	367	0.80	302	0.97
Beam No.	KNm·10	KNm·10		KNm·10	
I-1	2.222	1.929	1.15	1.910	1.16
I-2	2.104	1.929	1.09	1.862	1.13
I-3	1.784	1.929	0.92	1.624	1.10
I-4	1.784*	1.929	-	1.373	-
I-5	1.886	2.487	0.76	2.092	0.90
I-6	*	2.487	-	1.949	-
III-1	4.172	3.857	1.08	3.780	1.10
III-2	3.596	3.857	0.93	3.564	1.01
III-3	3.596	3.857	0.93	3.128	1.15
III-4	2.318*	3.857	-		-
III-5	4.129	3.868	1.07	3.791 <sup>Δ</sup>	1.09
III-6	3.703	3.868	0.96	3.133 <sup>Δ</sup>	1.18

\* cracking load

<sup>Δ</sup> n estimated at 2

The total test material comprises beams with 4, 8 and 16 longitudinal reinforcing bars and beams with 4 longitudinal reinforcing bars plus prestressed tendon.

Fig. 26-29 show the curves for the carrying capacity (in accordance with section 2.2) for beams with these numbers of longitudinal reinforcing bars (n = 1, 2 and 4), together with the results of the tests.

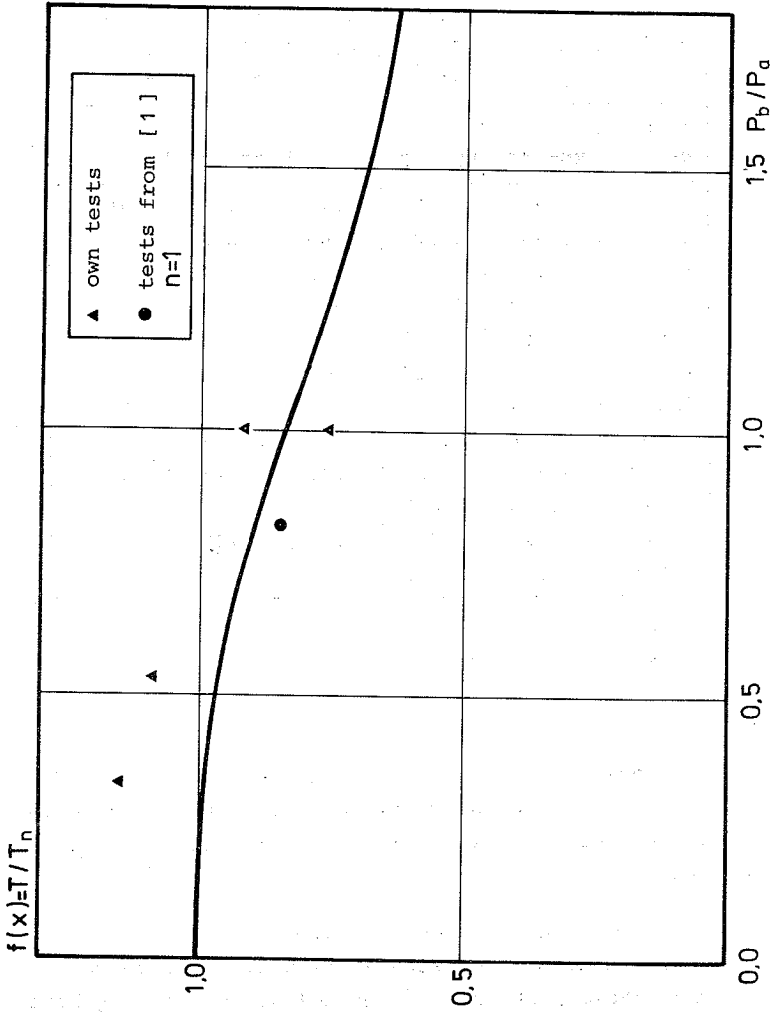


FIG. 26.

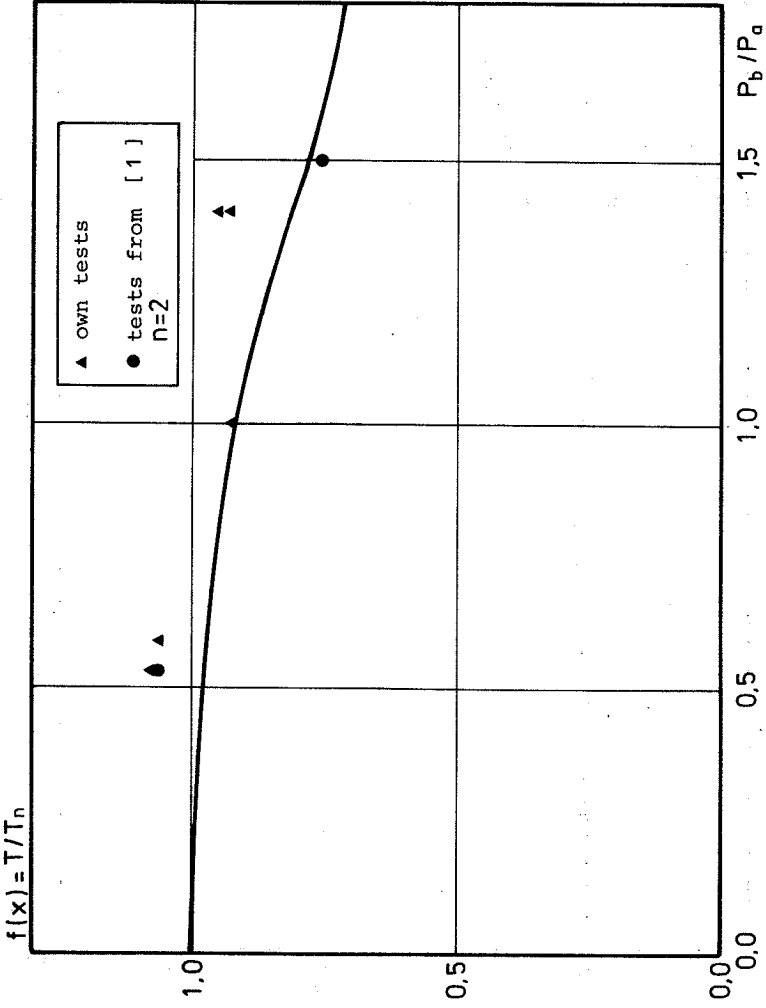


FIG. 27.

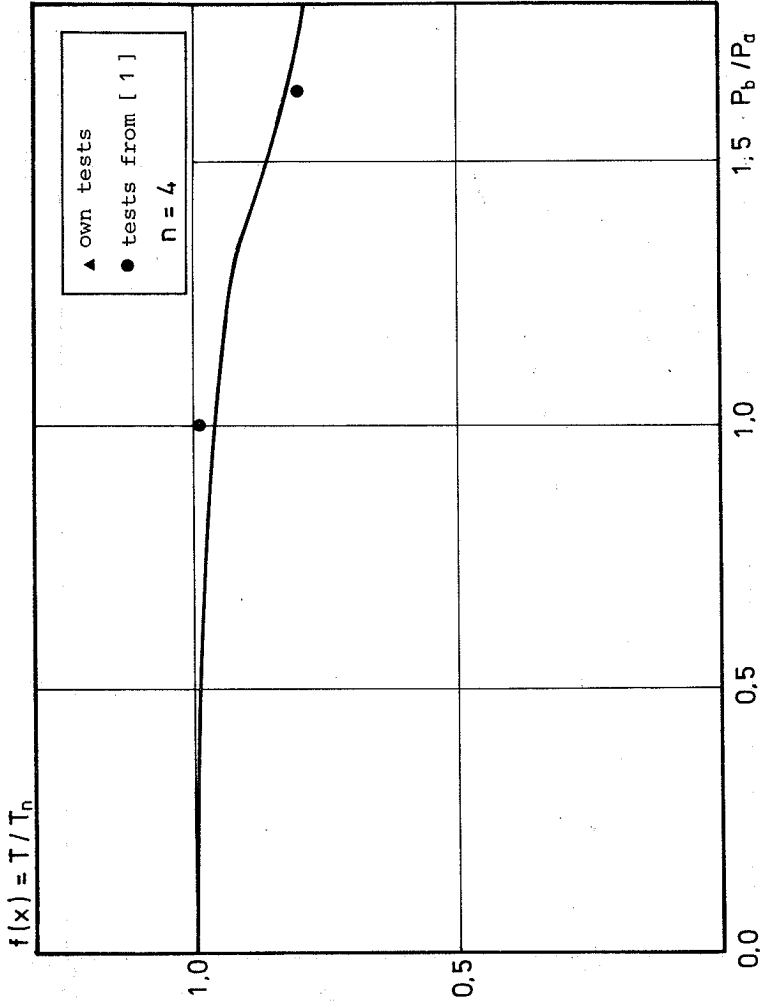


FIG. 28.

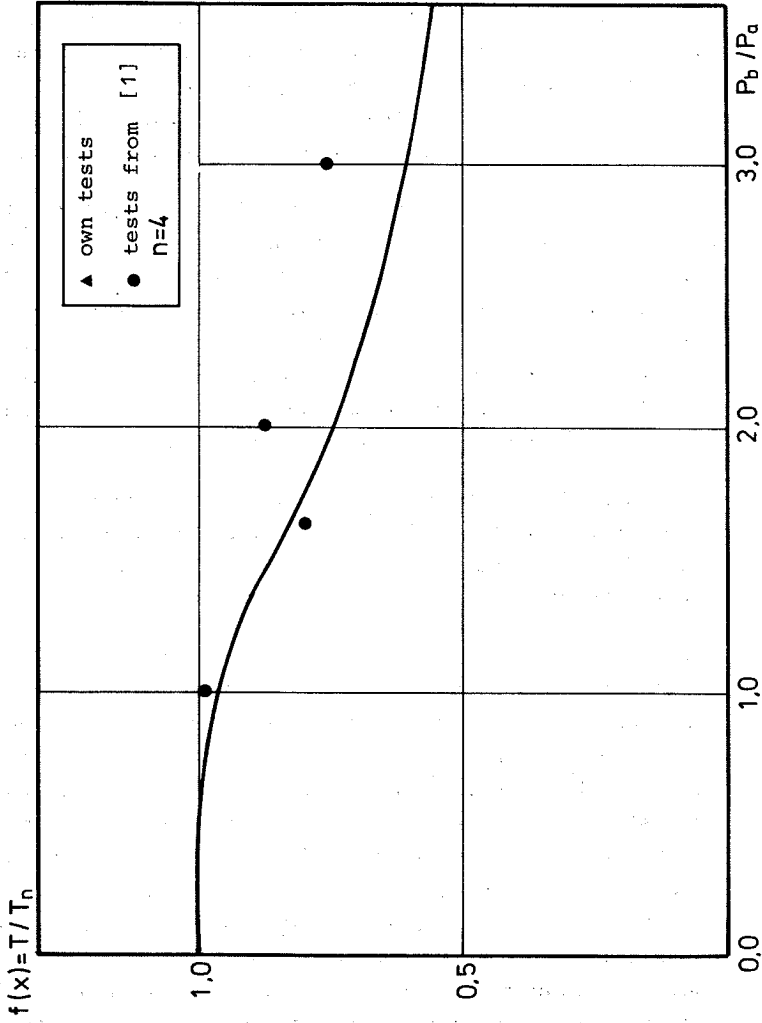


FIG. 29.

## 5. CONCLUSION

In this report it is demonstrated that, for normally reinforced beams in torsion, the effect of the stirrup spacing can be calculated by considering the interaction between concrete and reinforcement in a corner of a cross section. The correspondence between the observed and the anticipated values of the failure load (fig. 26 to fig. 29 ) seems to be satisfactory.

In particular, the results of the tests confirm that the carrying capacity of beams with a stirrup spacing that is less than the distance between two corner reinforcing bars decreases with increasing stirrup spacing. In addition, the tests also seem to confirm that the carrying capacity is not only dependent on the stirrup spacing, but also on the character of the reinforcing bars at the corners of the cross section.

The ultimate carrying capacity of the two partially prestressed beams II-5 and II-6 seems to show the same dependence on the stirrup spacing as for the traditionally reinforced beams.

With regard to fig. 29, better correspondence between experiment and theory could be achieved by assuming that only part of the compressive stresses in the concrete was transmitted to the longitudinal reinforcing bar and that the residue was transmitted directly to the stirrups through contact pressure. However, this only applies to the beams in fig. 29 (beams CO and C1), and as, furthermore, the stirrup arrangement is atypical (double and triple stirrups), with a considerably better possibility for direct force transmission than with a normal arrangement, the assumption in section 2.2 will be maintained (that the whole of the compression in the

concrete is transmitted to the longitudinal reinforcing bar in the corner). It is shown that the carrying capacity can be calculated by means of the following expression:

$$T = T_n \cdot f \left( \frac{P_b}{P_a} \right)$$

where,

$T_n$  = the carrying capacity calculated in accordance with the lattice analogy method

$$= 2 \cdot a \cdot b \cdot \sqrt{n_{xa} \cdot n_{ya}}$$

where:

$a, b$  = the side lengths of the rectangle formed by the longitudinal reinforcement,

$n_{xa}$  = the force in the reinforcement per unit length (in the longitudinal direction),

$n_{ya}$  = the force in the reinforcement per unit length (in the stirrup direction)

$$f \left( \frac{P_b}{P_a} \right) = \begin{cases} \sqrt{\frac{(n-1) + \sqrt{1 - \frac{1}{2} \left( \frac{P_b}{P_a} \right)^2}}{n}} & ; \quad P_b \leq \gamma \cdot P_a \\ \sqrt{\frac{(n-1) + \sqrt{1 - \frac{1}{2} \gamma^2 \frac{P_a}{P_b}}}{n}} & ; \quad P_b \geq \gamma \cdot P_a \end{cases} \text{ for}$$

where:  $1 \leq \gamma < \sqrt{2}$

$$\gamma = \sqrt{1 - \frac{1}{4}(n-1)^2 + \frac{1}{4}(n-1) \sqrt{(n-1)^2 + 8}}$$

$n$  = the ratio between the total force in the reinforcement in the longitudinal direction and the sum of the force in the corner reinforcement,



$P_b$  = the yield force in a stirrup,

$P_a$  = the yield force in a corner reinforcing bar.

Furthermore, it has been observed that the mode of failure changes at stirrup spacings greater than the distance between two corner bars, to a failure pattern analogous to that for unreinforced beams. Beams with such a failure pattern have a very low ultimate strength and should therefore be avoided.

The theory developed here can be used as follows to formulate simple design rules:

An increase in the ratio  $\frac{P_b}{P_a}$  beyond the value  $\gamma$ , where  $\gamma$  is determined from the expression on page 45, will not result in yielding in the stirrups, and it is therefore appropriate to limit  $P_b$  to the value  $\gamma \cdot P_a$ .

$\gamma$  assumes only values between 1 and  $\sqrt{2}$ , and as a  $\gamma$ -value near  $\sqrt{2}$  would give big deflections of the corner bars, it is proposed that the value of  $\gamma$  be put at 1 and thus that

$$P_b \leq P_a$$

be prescribed.

For beams with 8 or more longitudinal reinforcing bars of the same dimension (and  $n_{xa} = n_{ya}$ ), this requirement is synonymous with a stirrup spacing of  $s \leq \frac{1}{4}(a+b)$ . If this latter requirement is extended to apply to all reinforcing bars, we get:

$$P_b \leq P_a$$

$$s \leq \frac{1}{4}(a+b)$$

which means that we have limited the reduction in the bearing capacity to maximum 3% (see curves for bearing

capacity, fig. 26 to fig. 29). In addition, it must be checked, with a reasonable degree of certainty, that no crack can form that is not crossed by a stirrup. This requirement can possibly be included by requiring instead that:

$$P_b \leq P_a$$

$$s \leq \frac{1}{2} \min(a,b)$$

## APPENDIX

In addition to photos of the crack patterns observed in the tests, this appendix contains the following six curves for each beam:

### 1. Loading histogram

abscissa: time in minutes from commencement of test  
ordinate: torsional moment  
comments: owing to the fact that the dead load of the beam contributes to the load, the curve does not start at (0,0).

### 2. Rotations

abscissa: mutual placing of the angular potentiometers (indicated by vertical lines)  
ordinate: angle of rotation in relation to 1st measuring point  
comments: each corresponds to one loading phase, the magnitude of which (in Mpm) is given on the right of each curve.

### 3. Stress-strain diagrams

abscissa: the rotation between measuring points 2 and 5  
ordinate: torsional moment.

### 4. Strains in reinforcement

abscissa: torsional moment  
ordinate: mean strain from one pair of gauges.

5. Differential strains

abscissa: torsional moment  
ordinate: difference between one pair of gauges

6. Forces in reinforcement

abscissa: torsional moment  
ordinate: force in one reinforcing bar  
comments: the yield stresses for the various bars are given on the left of the figures.

The sides of the beams are numbered as follows:

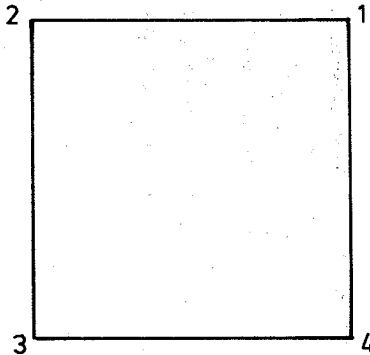
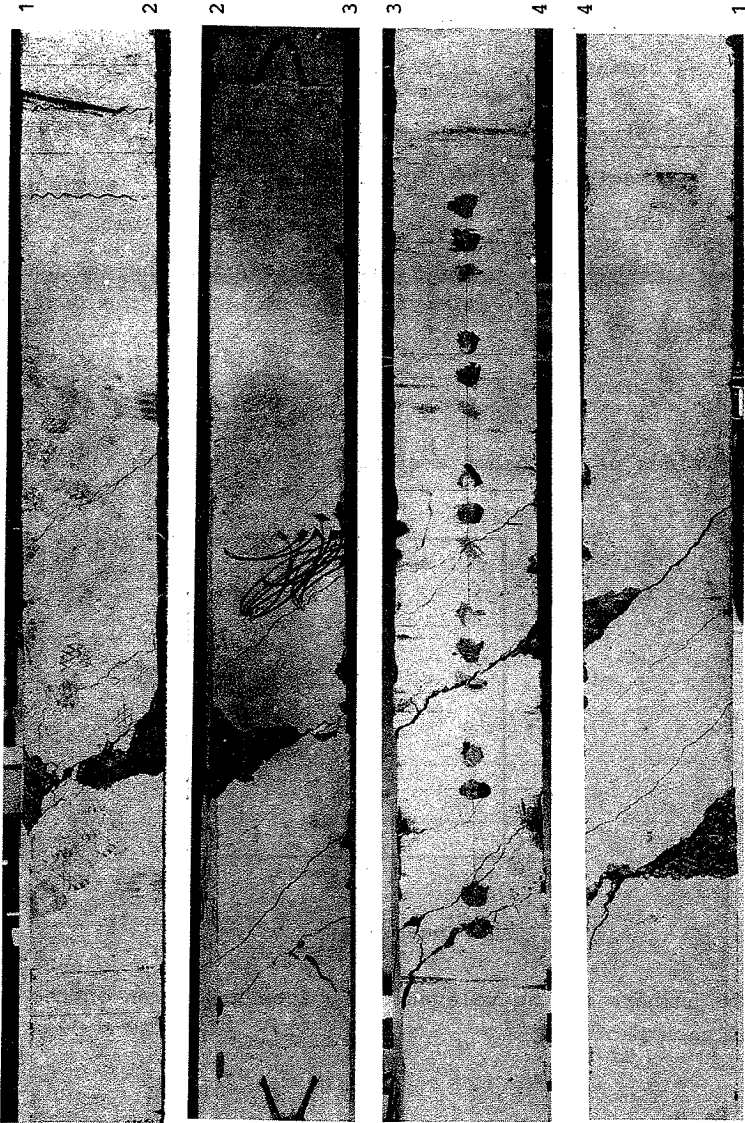


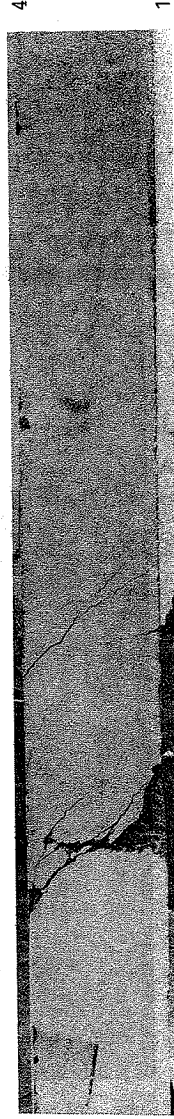
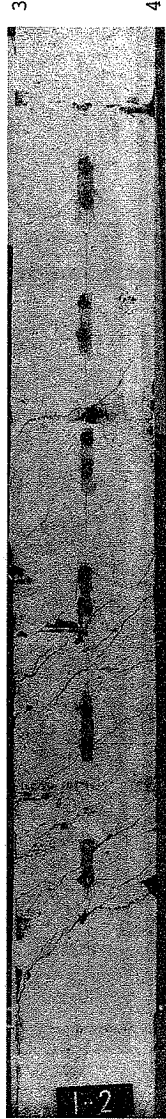
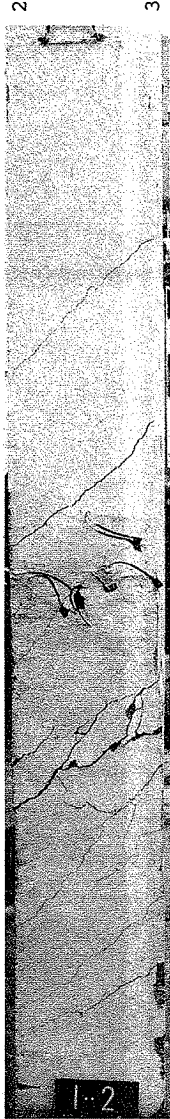
Fig. 30. Beam seen from end

The numbers of the relevant side face are given on the right of each photo.

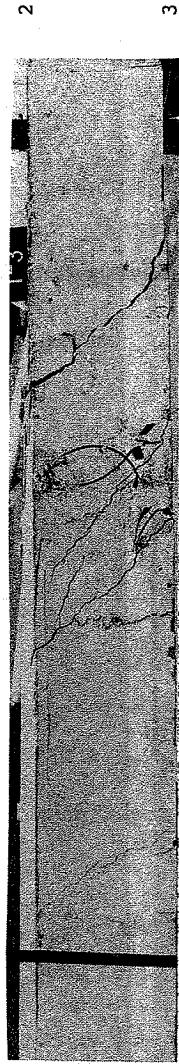
BEAM NO. I-1



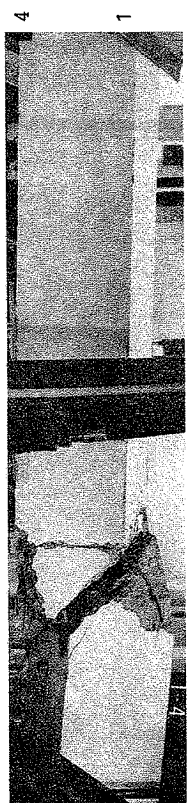
BEAM NO. I-2



BEAM NO. I-3

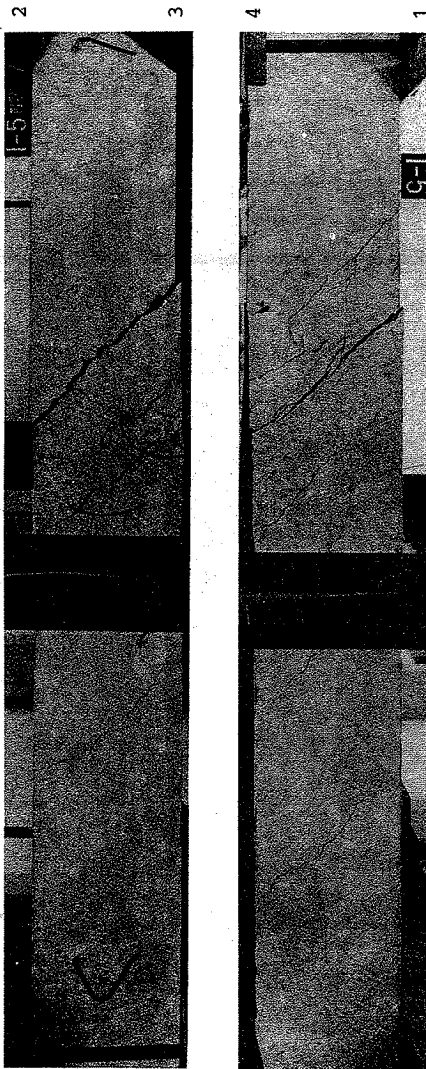


BEAM NO. I-4

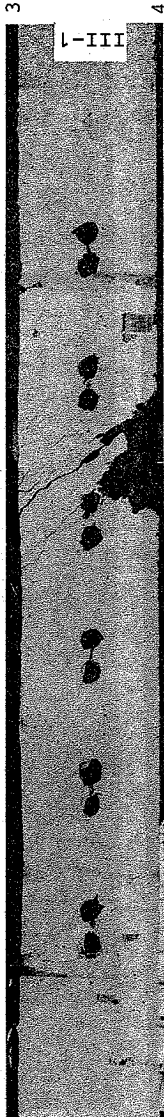




BEAM NO. I-5



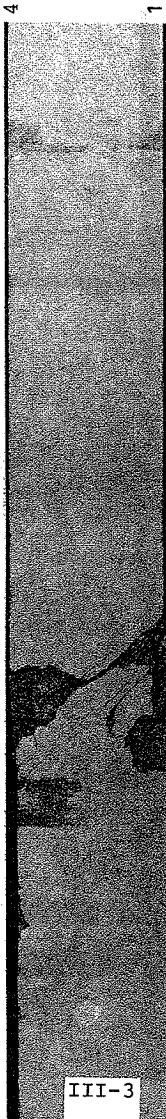
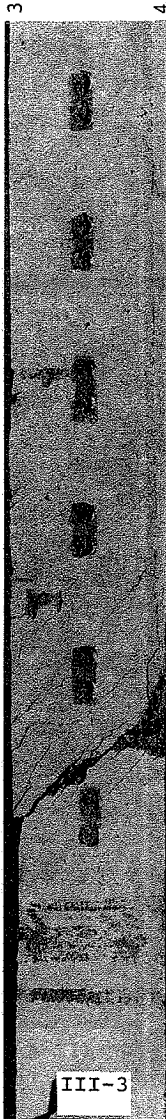
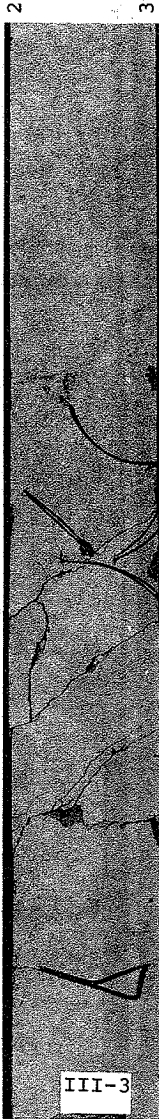
BEAM NO. III-1



BEAM NO. III-2

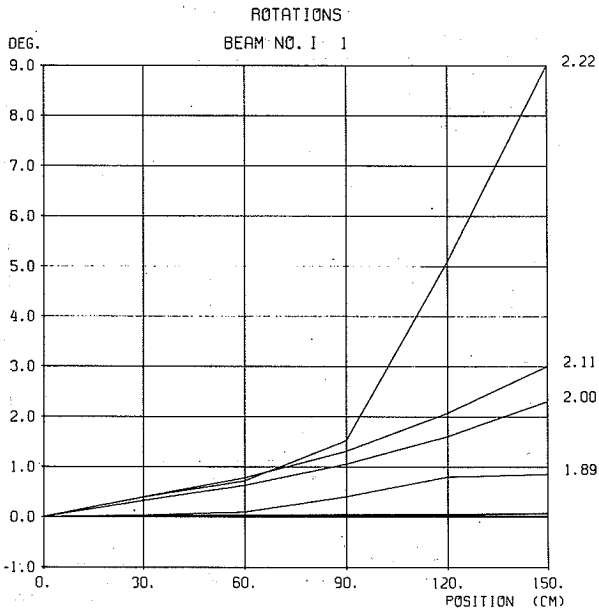
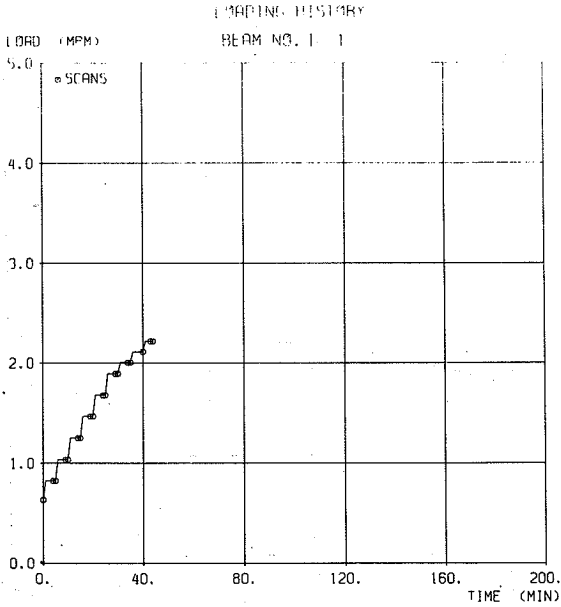


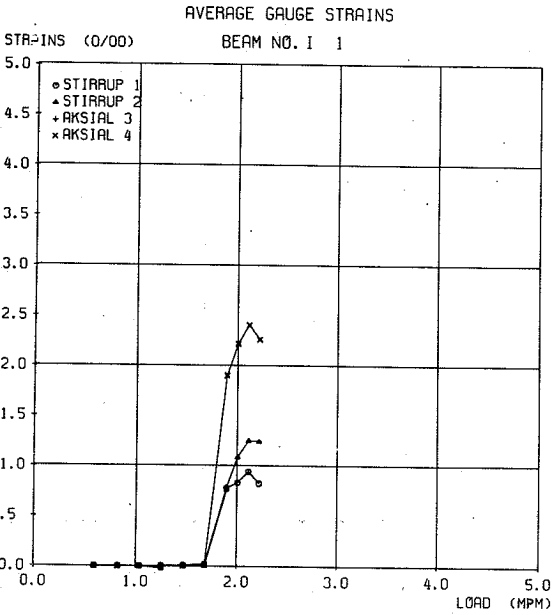
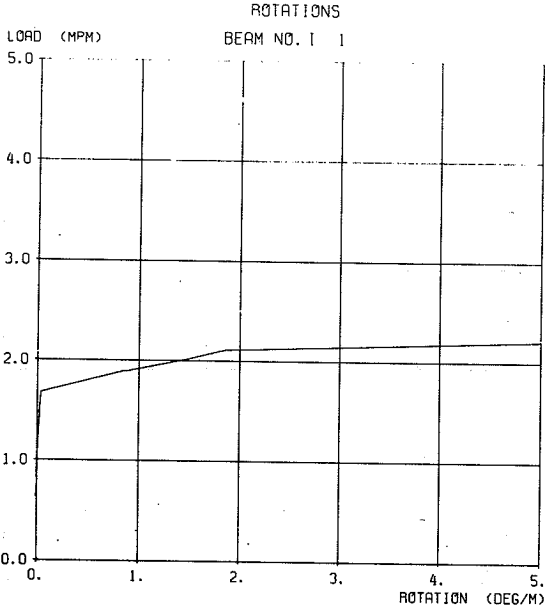
BEAM NO. III-3



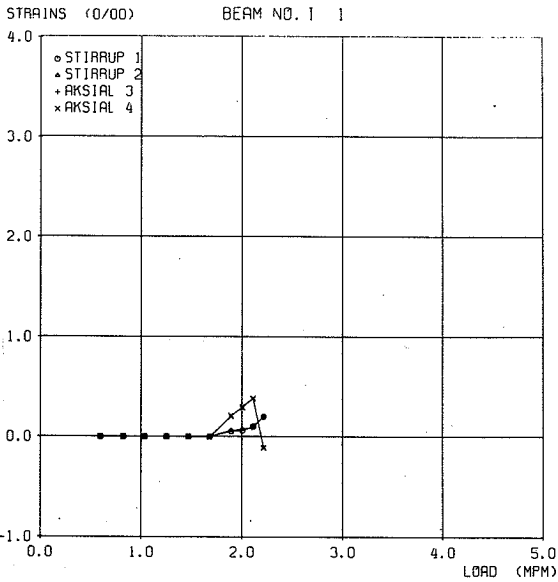
BEAM NO. III-4



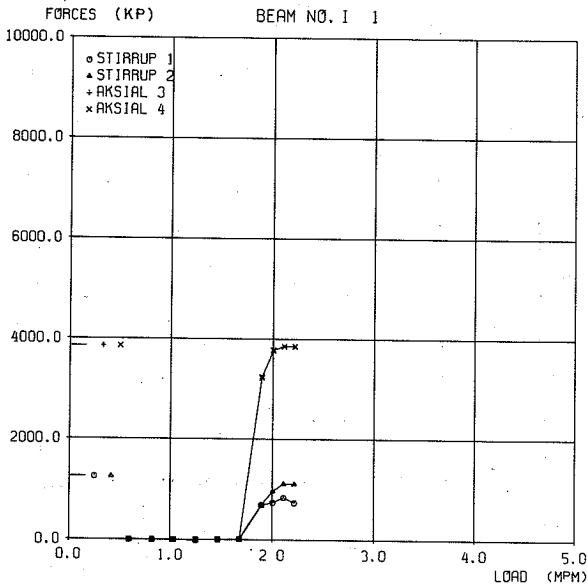




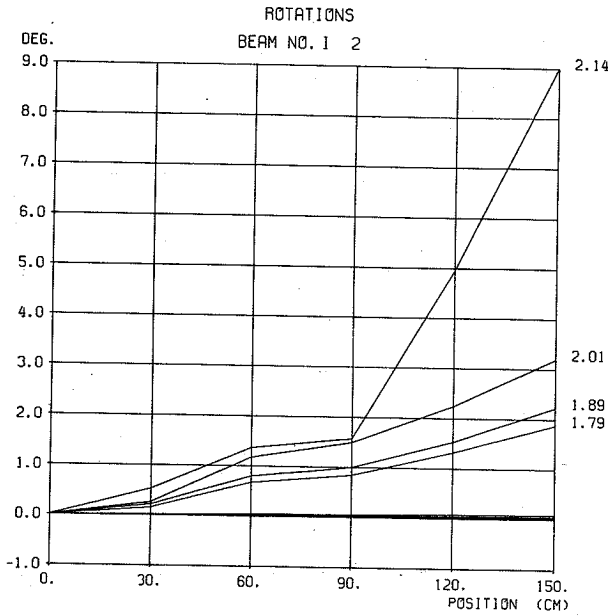
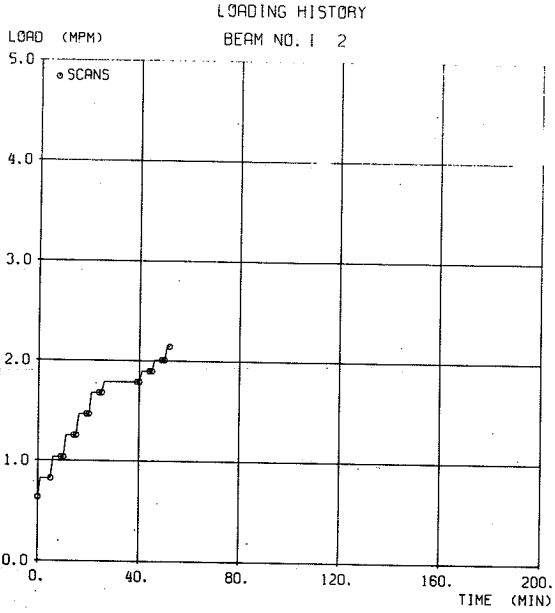
DIFFERENCE BETWEEN GAUGE STRAINS

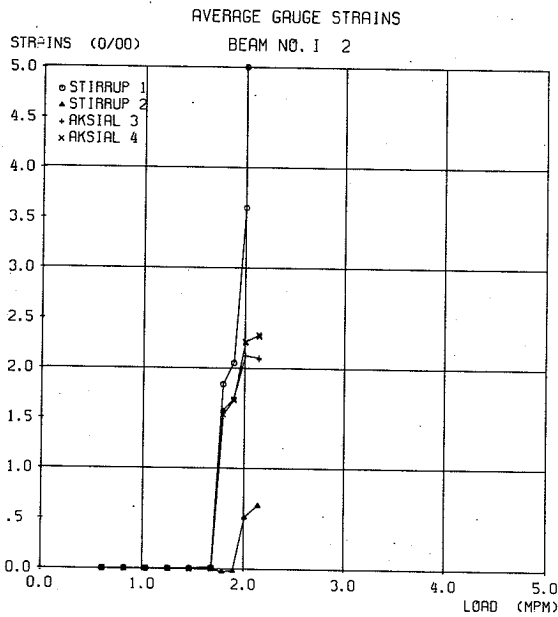
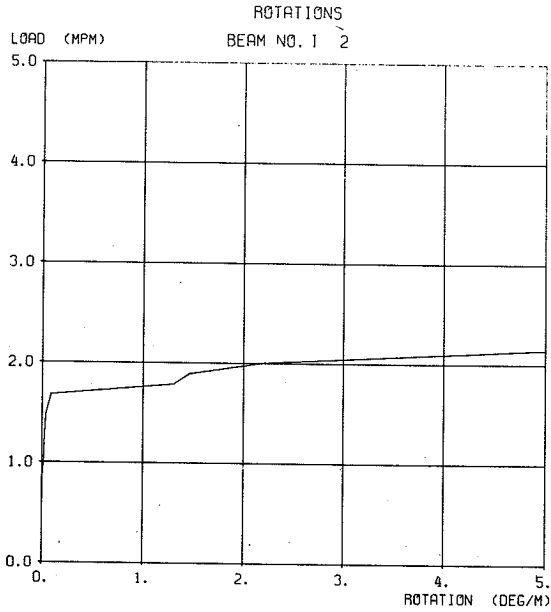


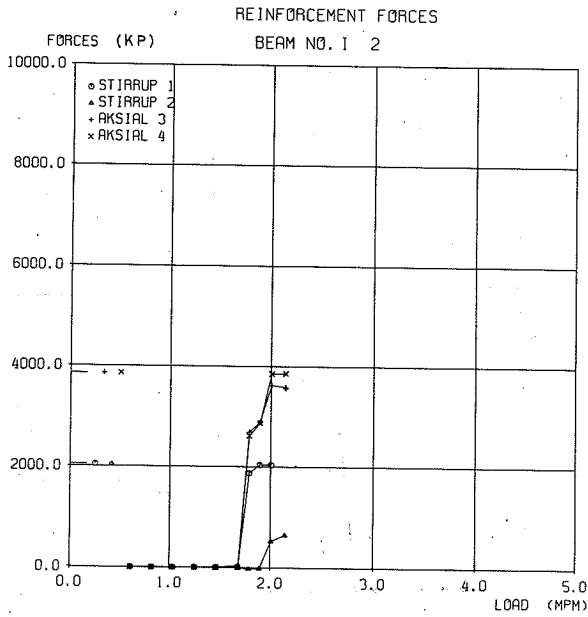
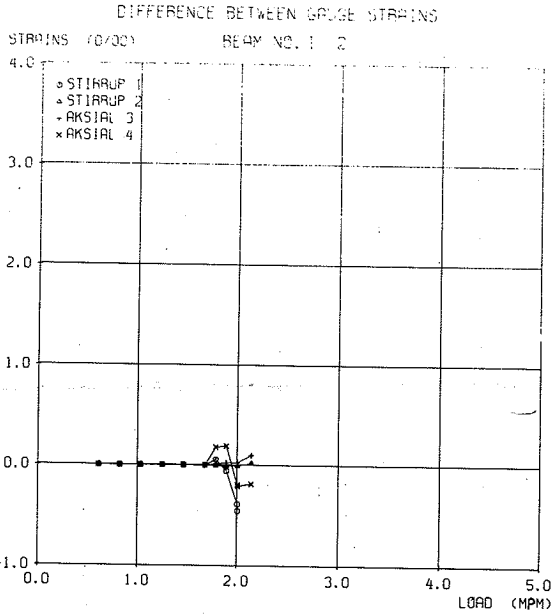
REINFORCEMENT FORCES



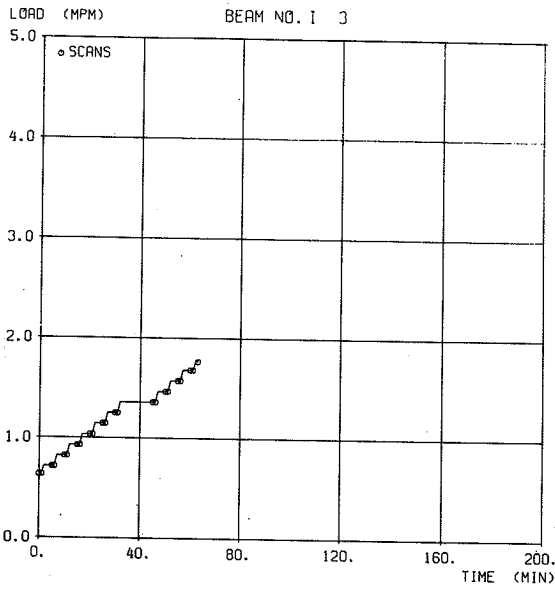




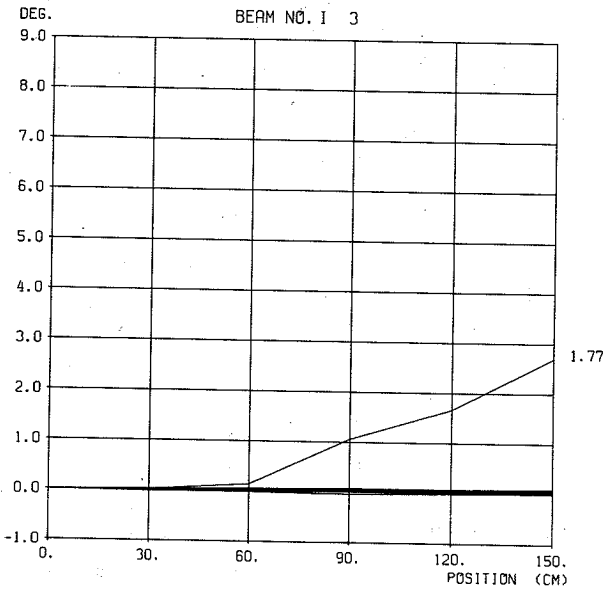


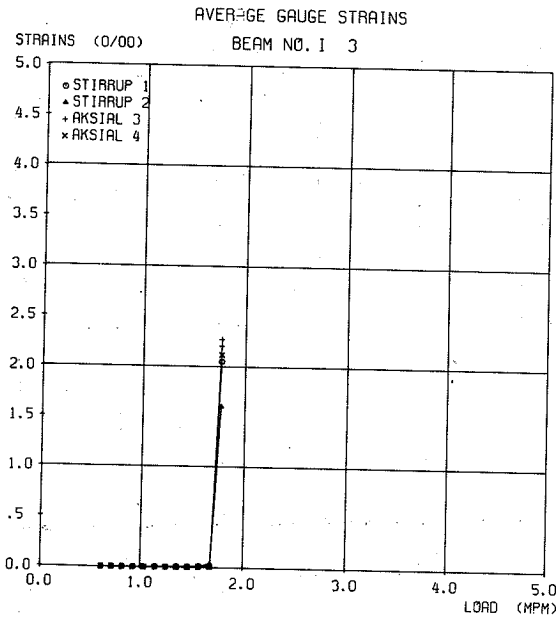
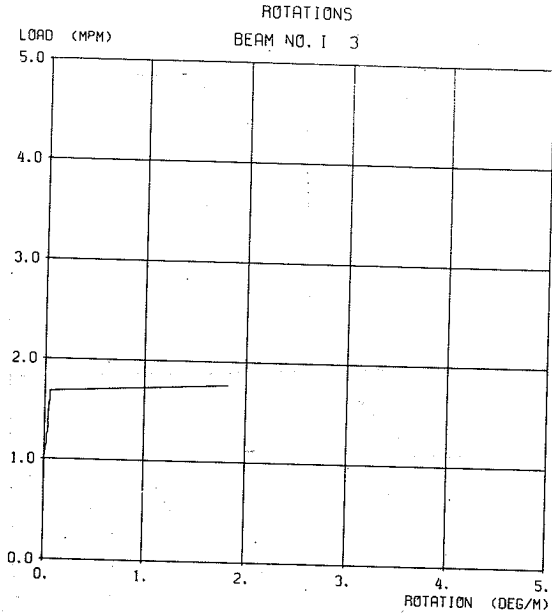


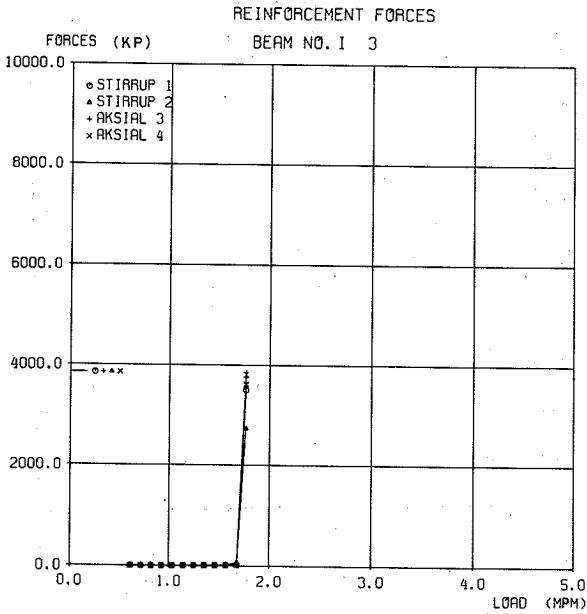
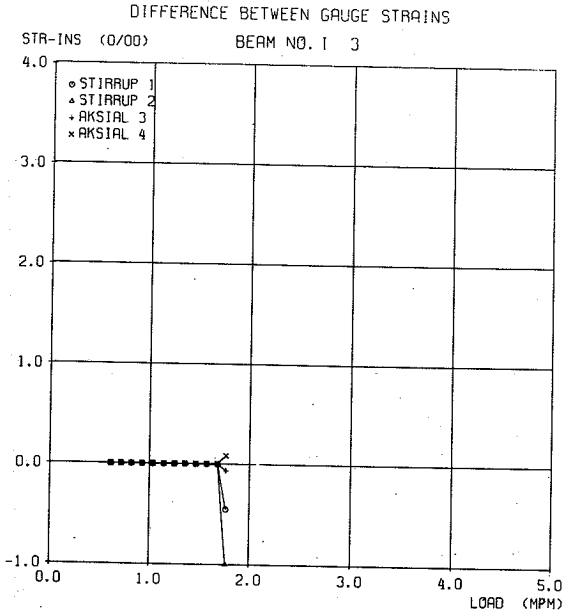
LOADING HISTORY



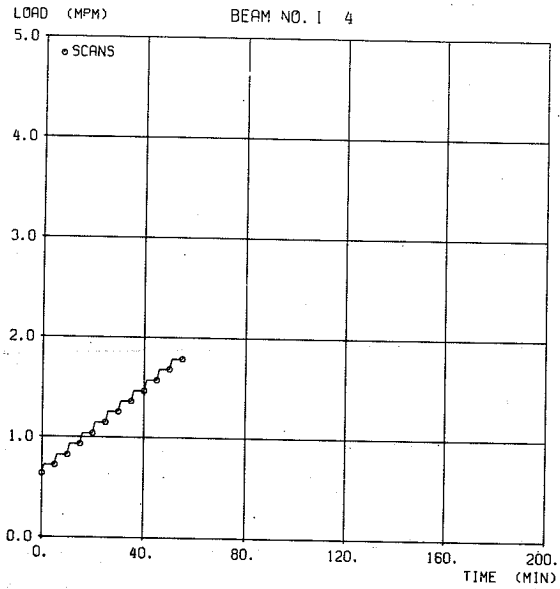
ROTATIONS



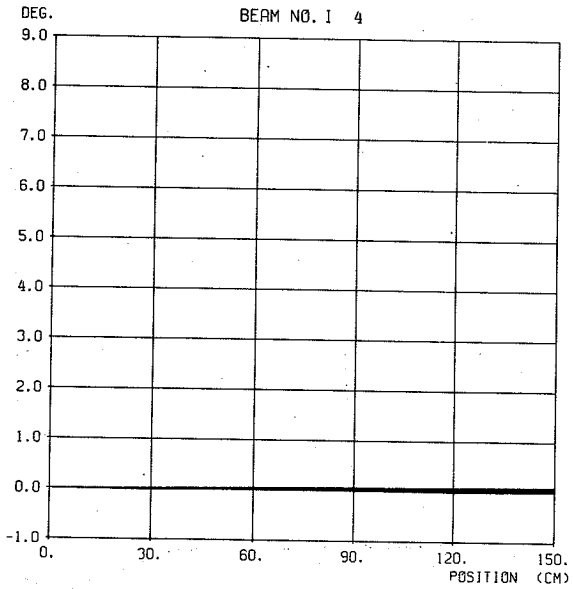


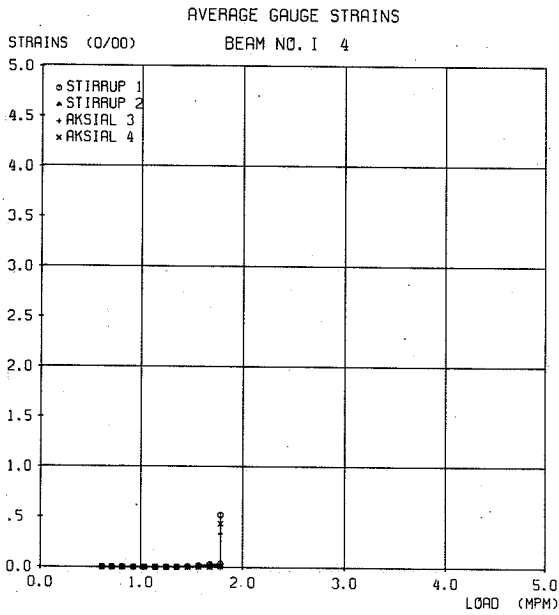
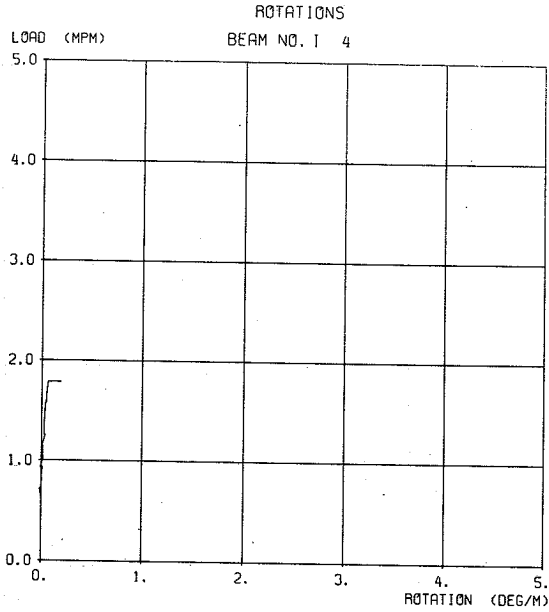


LOADING HISTORY  
BEAM NO. I 4

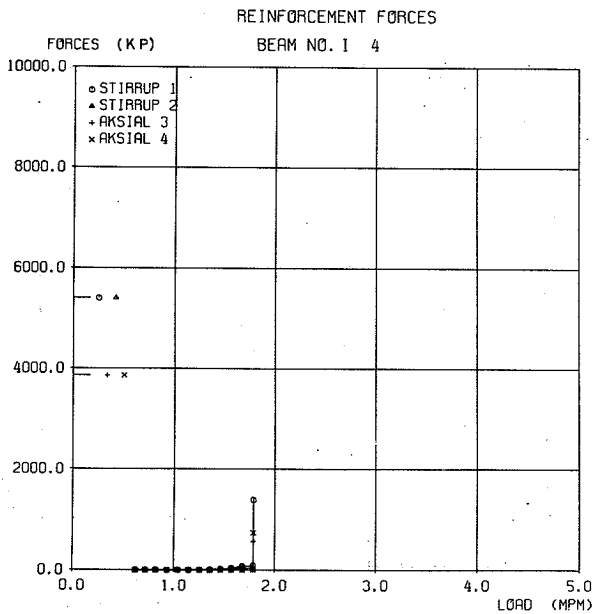
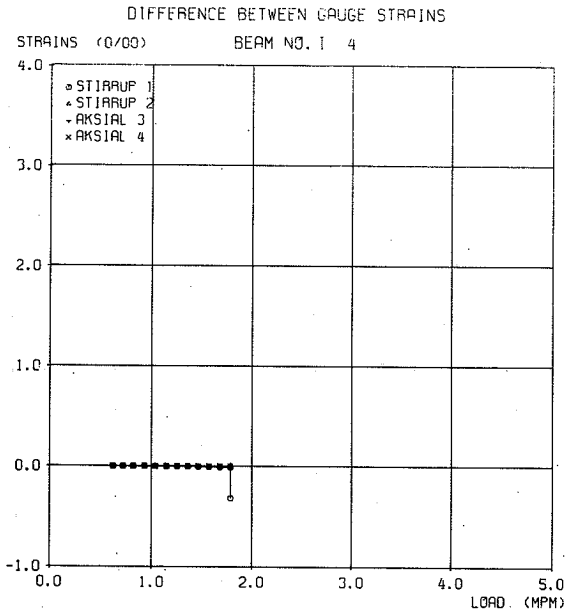


ROTATIONS  
BEAM NO. I 4



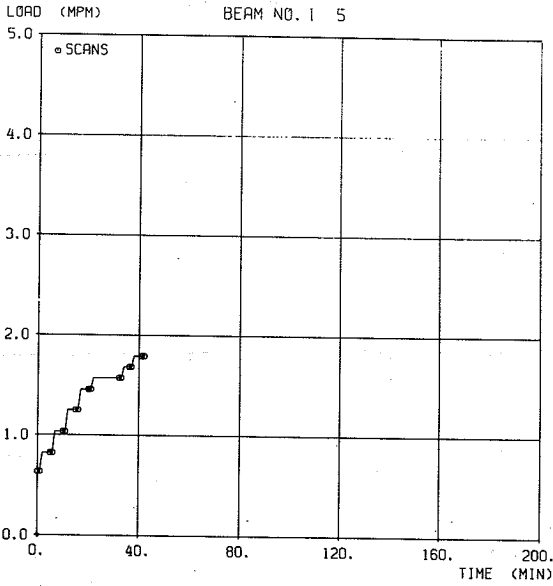






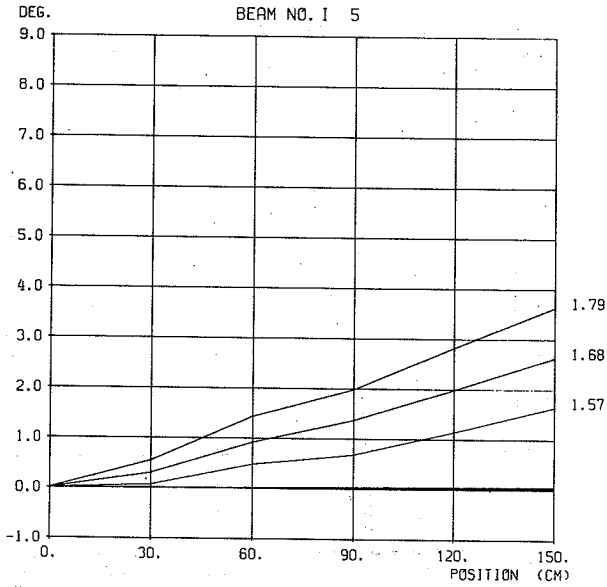
LOADING HISTORY

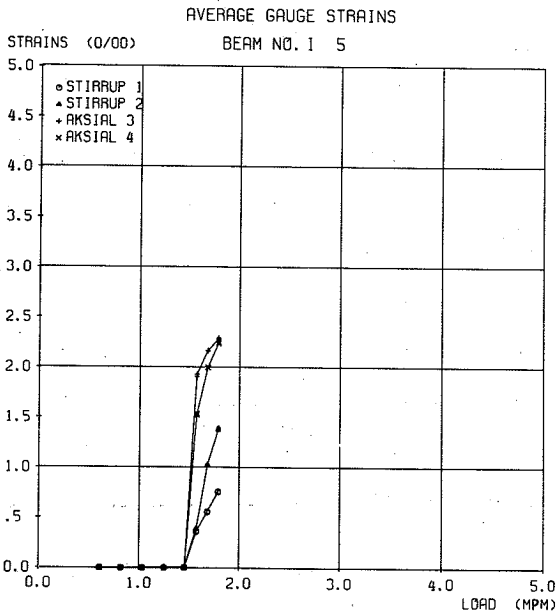
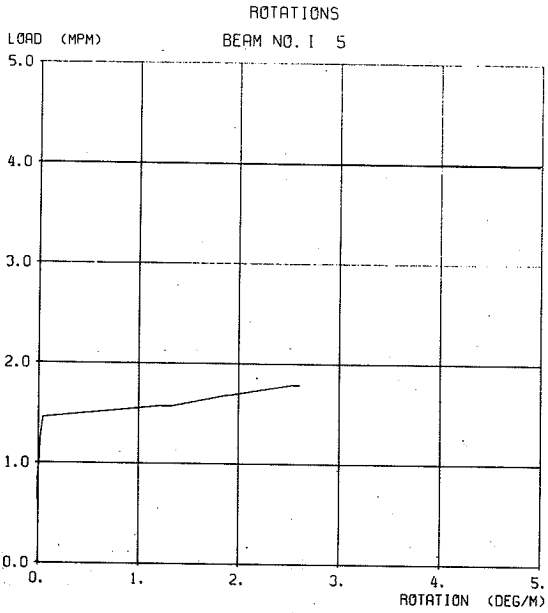
BEAM NO. I 5



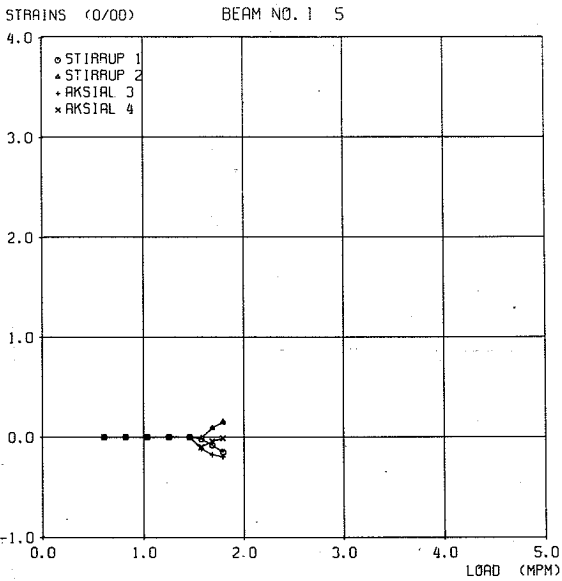
ROTATIONS

BEAM NO. I 5

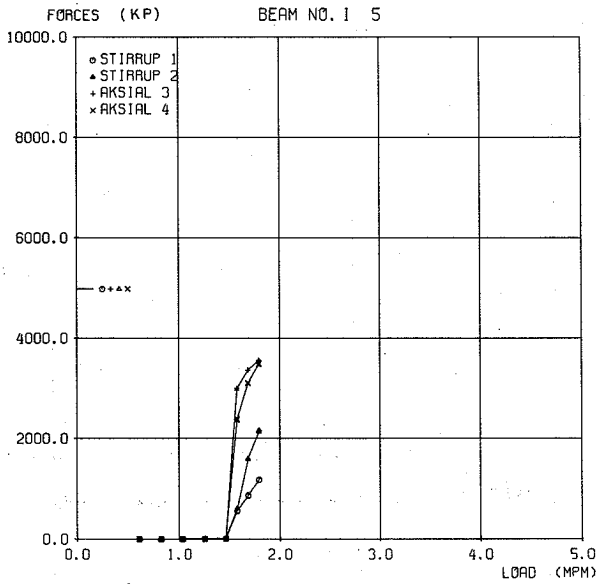




DIFFERENCE BETWEEN GAUGE STRAINS

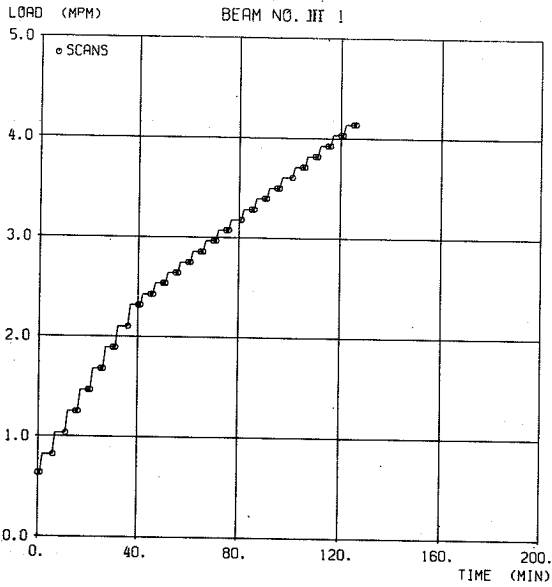


REINFORCEMENT FORCES



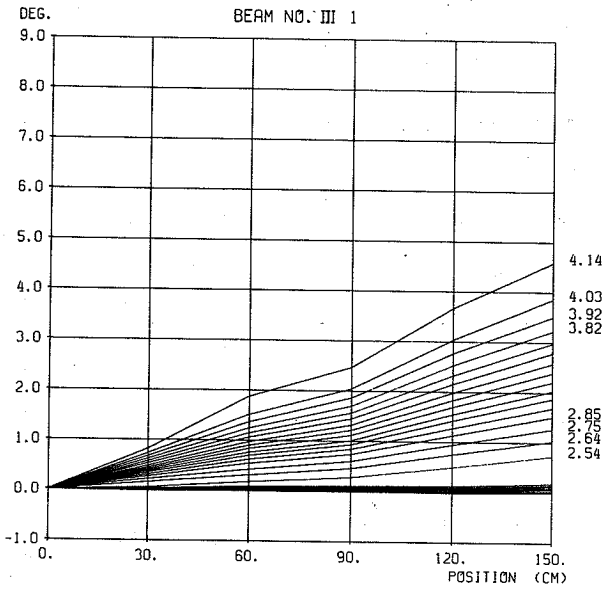
### LOADING HISTORY

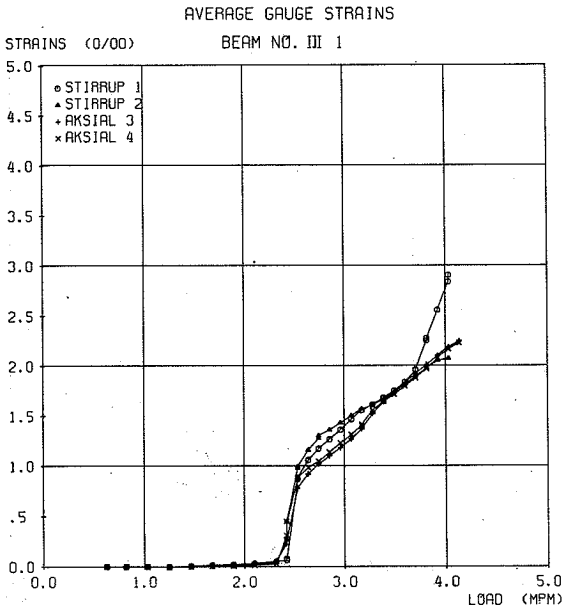
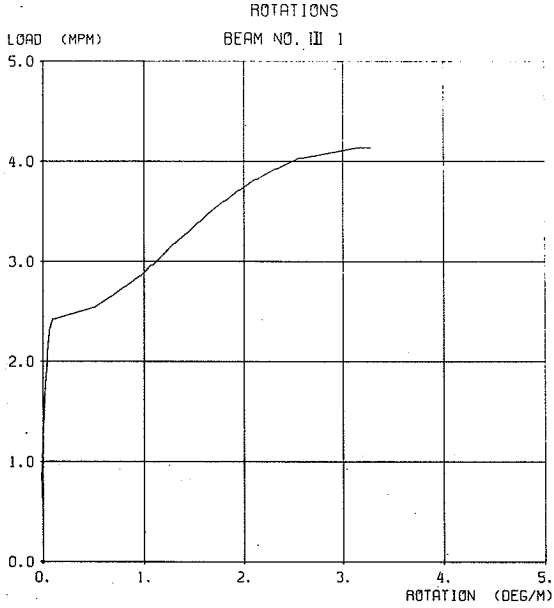
BEAM NO. III 1

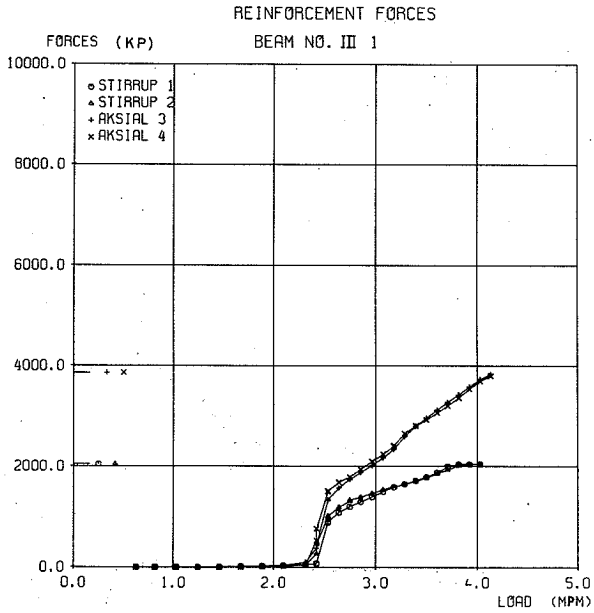
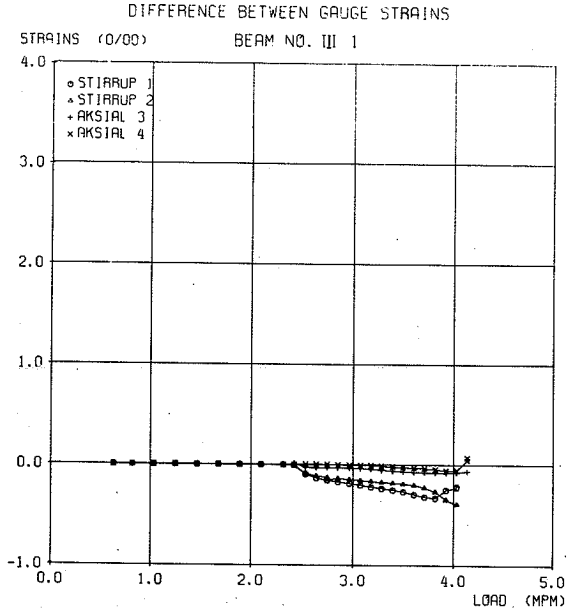


### ROTATIONS

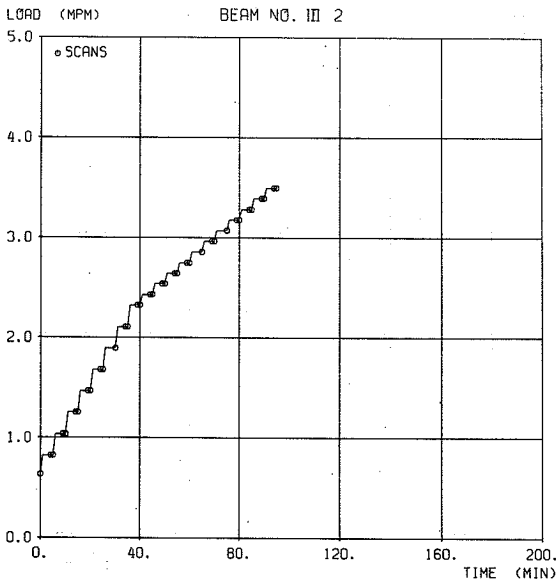
BEAM NO. III 1



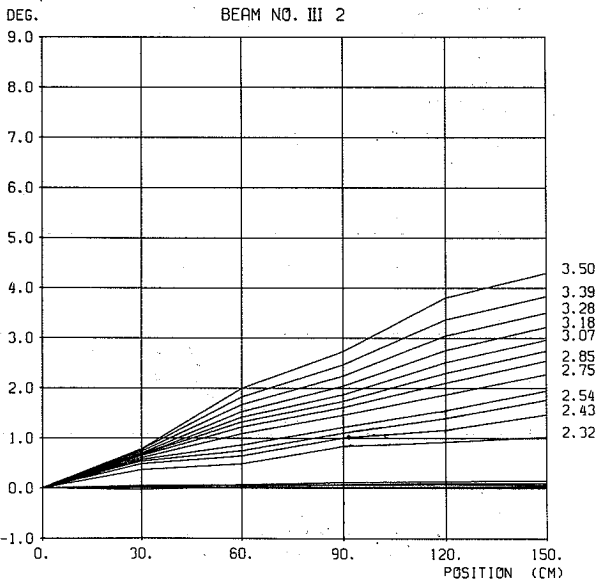




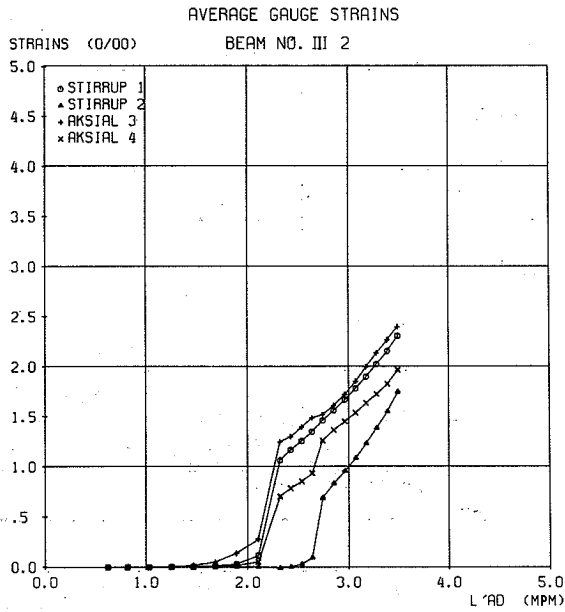
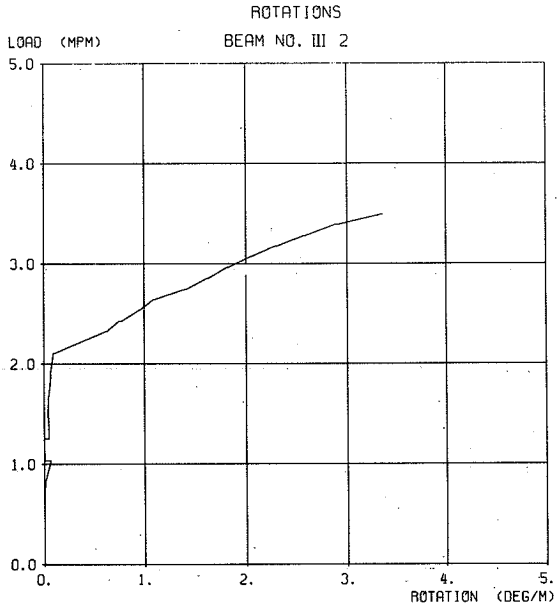
LOADING HISTORY



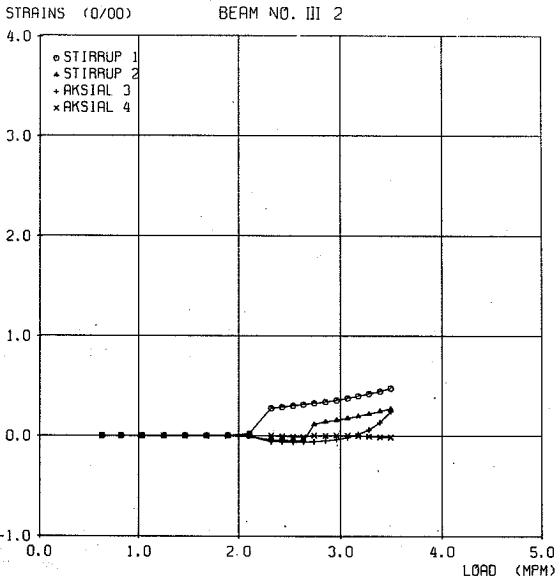
ROTATIONS



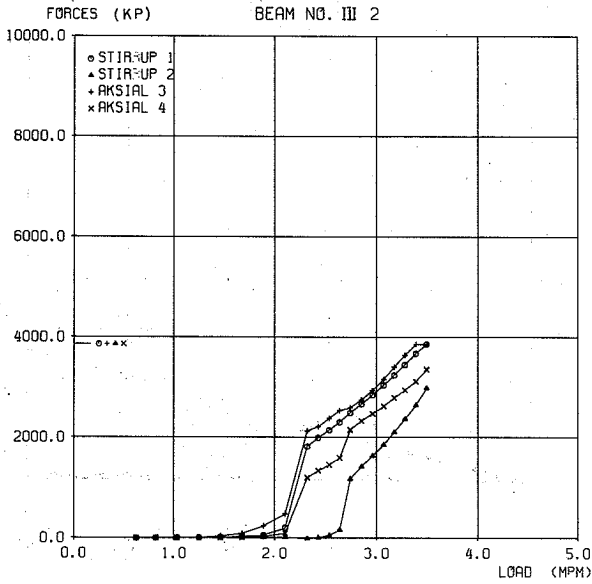




DIFFERENCE BETWEEN GAUGE STRAINS

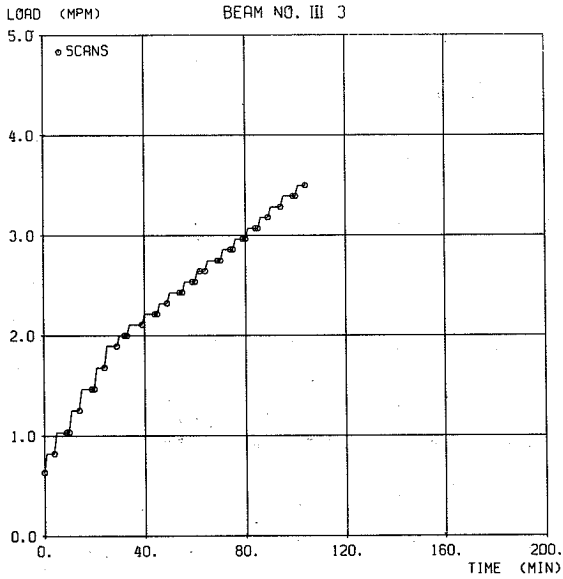


REINFORCEMENT FORCES



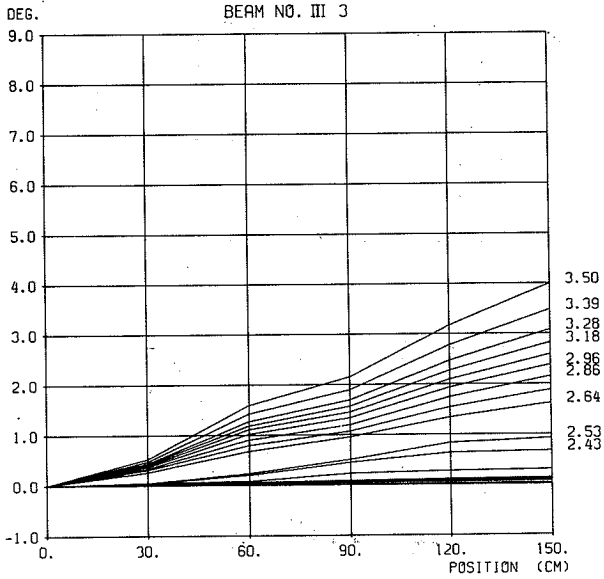
LOADING HISTORY

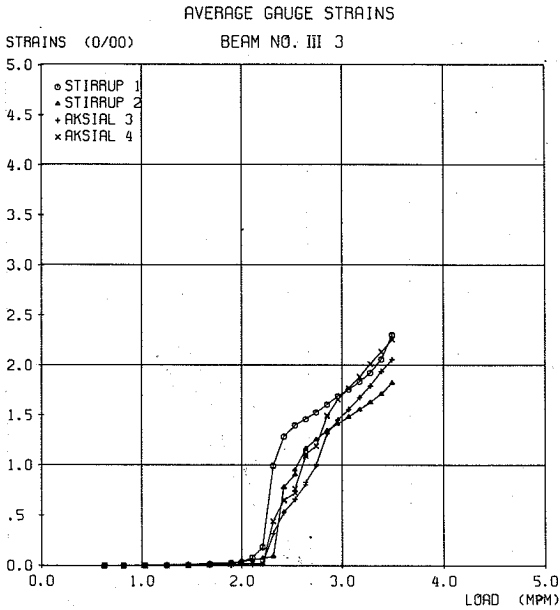
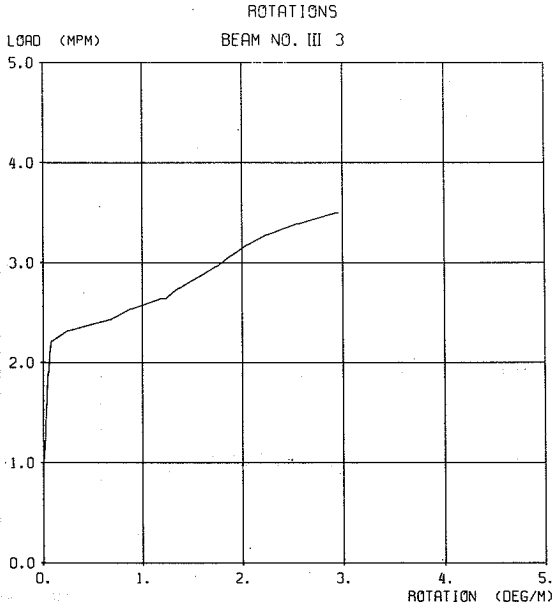
BEAM NO. III 3



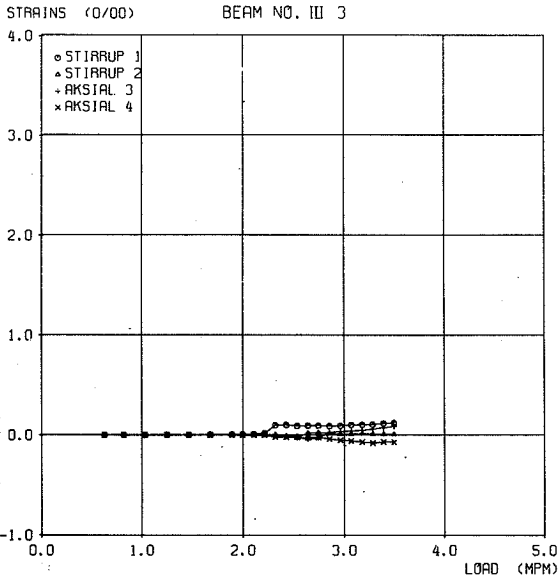
ROTATIONS

BEAM NO. III 3

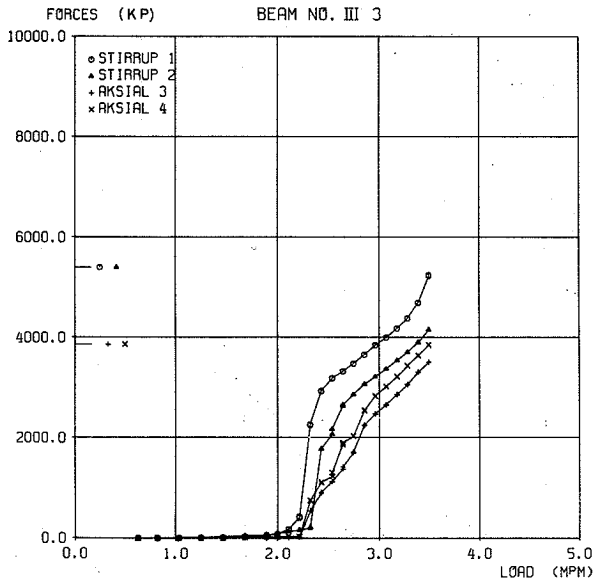




DIFFERENCE BETWEEN GAUGE STRAINS

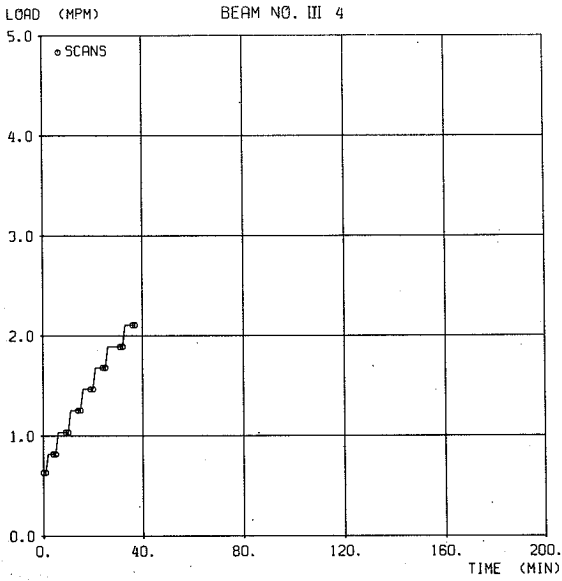


REINFORCEMENT FORCES



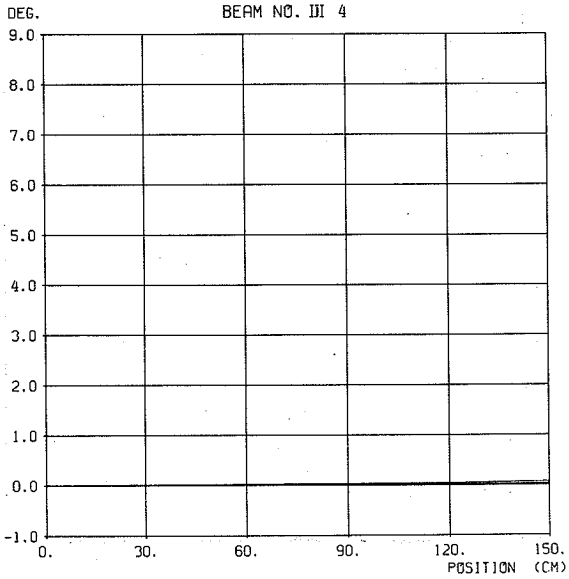
LOADING HISTORY

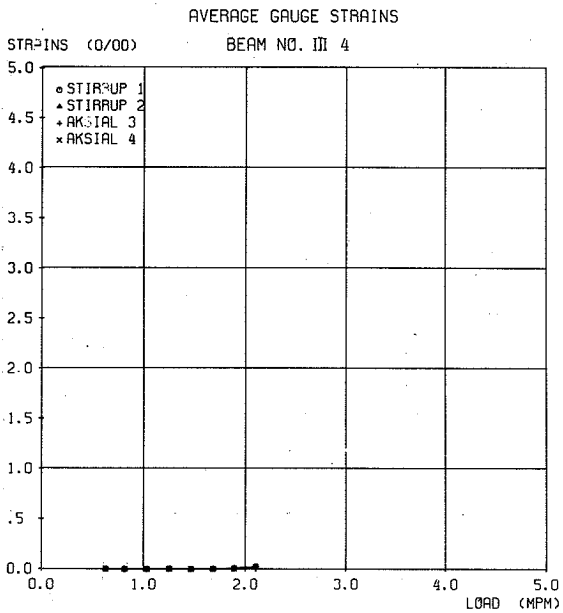
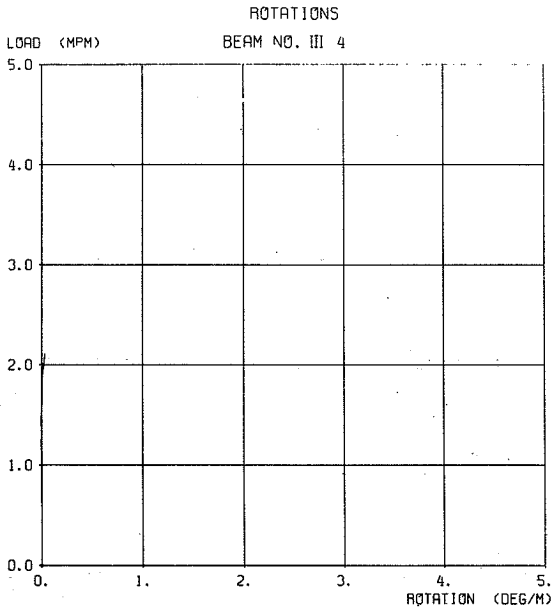
BEAM NO. III 4



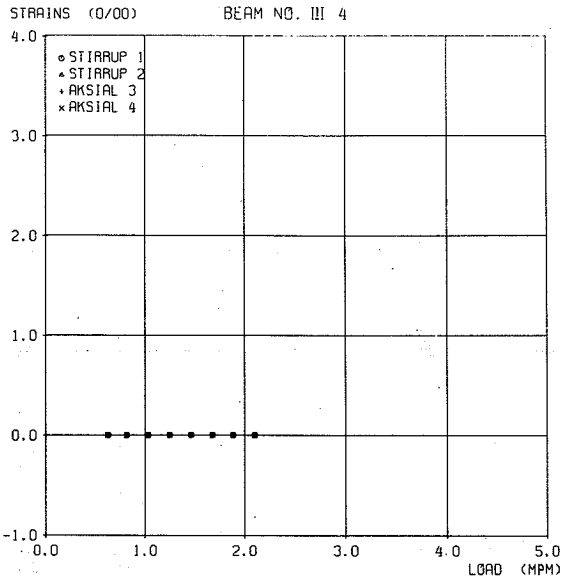
ROTATIONS

BEAM NO. III 4

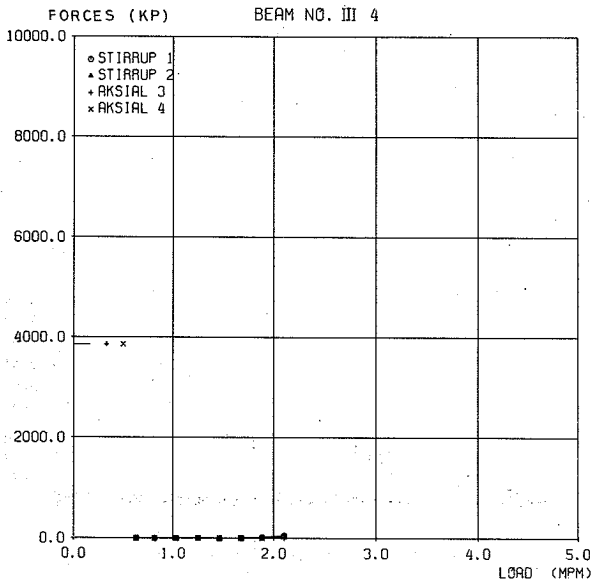




DIFFERENCE BETWEEN GAUGE STRAINS



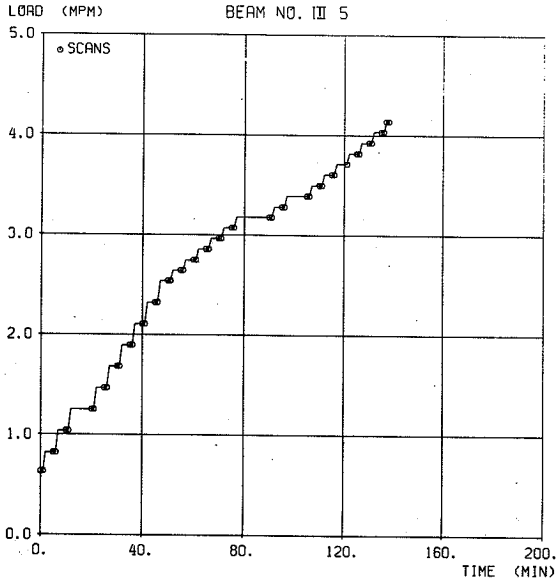
REINFORCEMENT FORCES





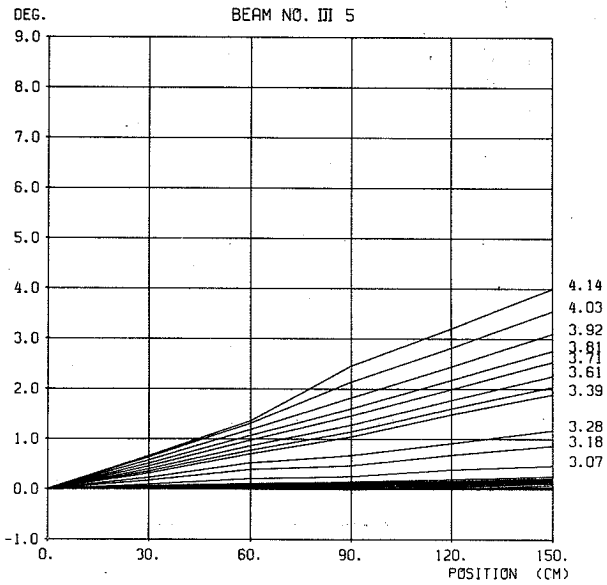
LOADING HISTORY

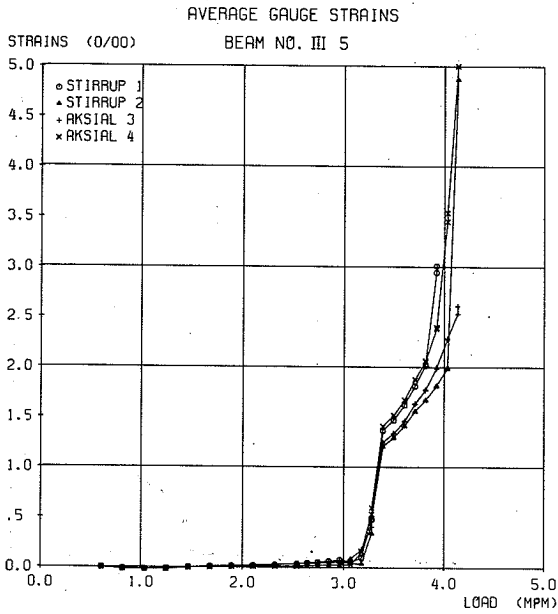
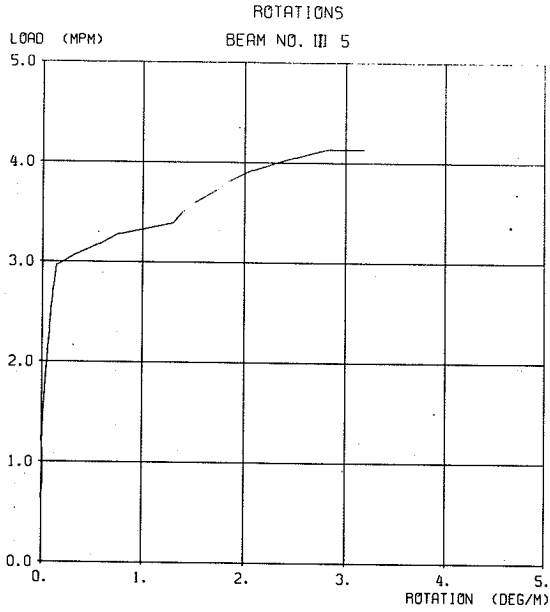
BEAM NO. III 5



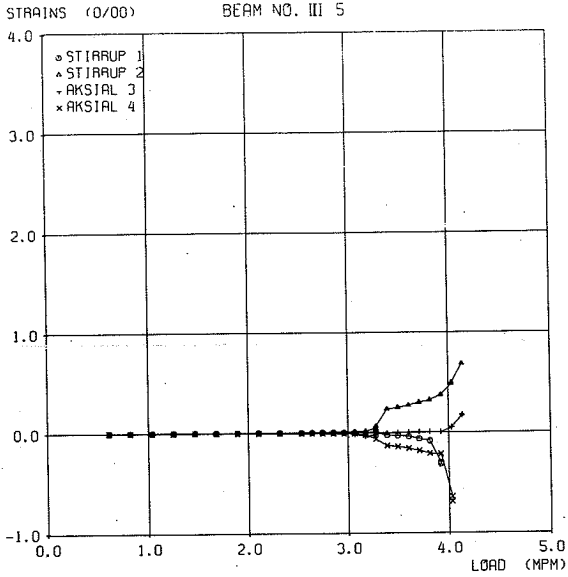
ROTATIONS

BEAM NO. III 5

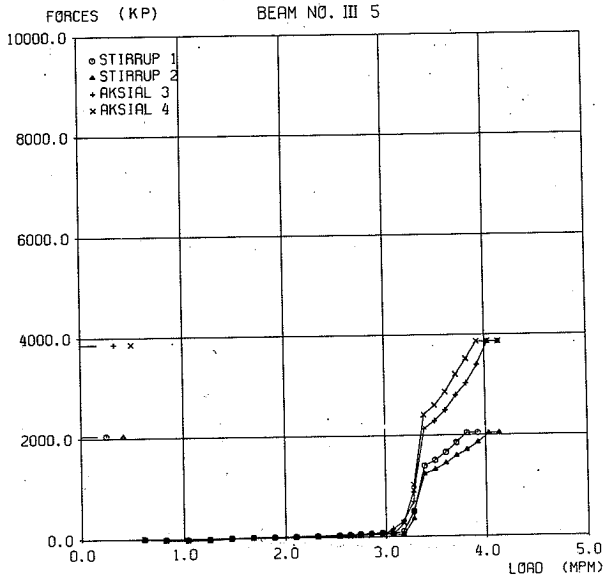




DIFFERENCE BETWEEN GAUGE STRAINS

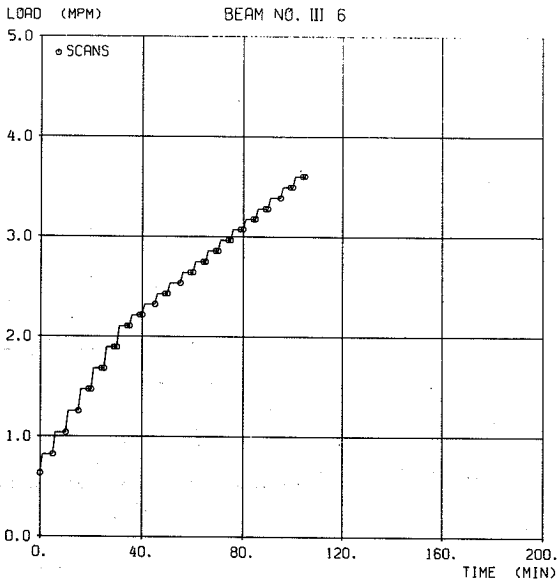


REINFORCEMENT FORCES



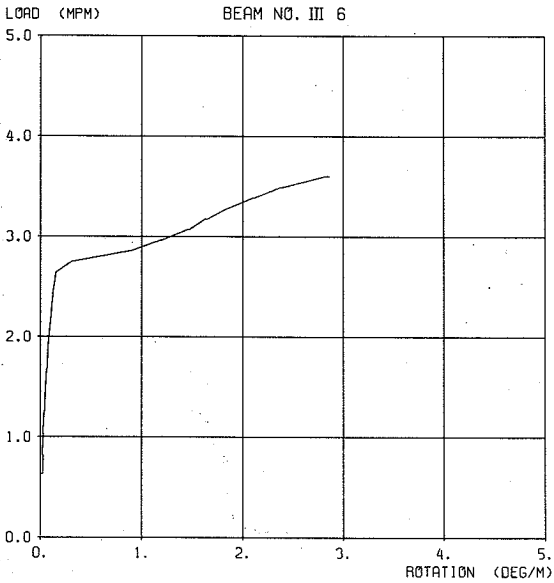
LOADING HISTORY

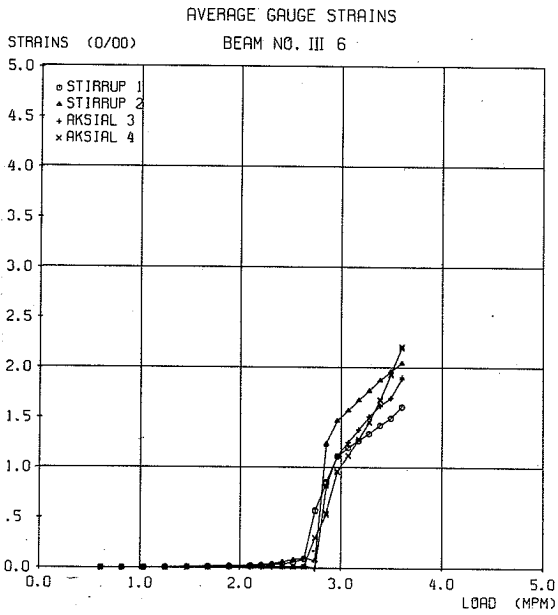
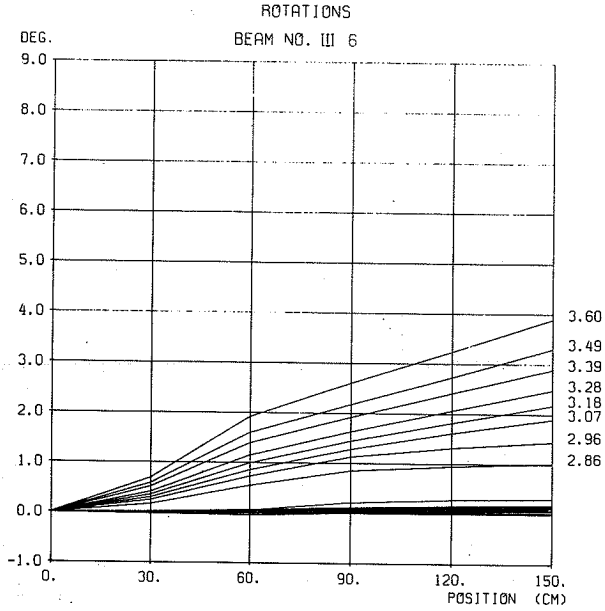
BEAM NO. III 6

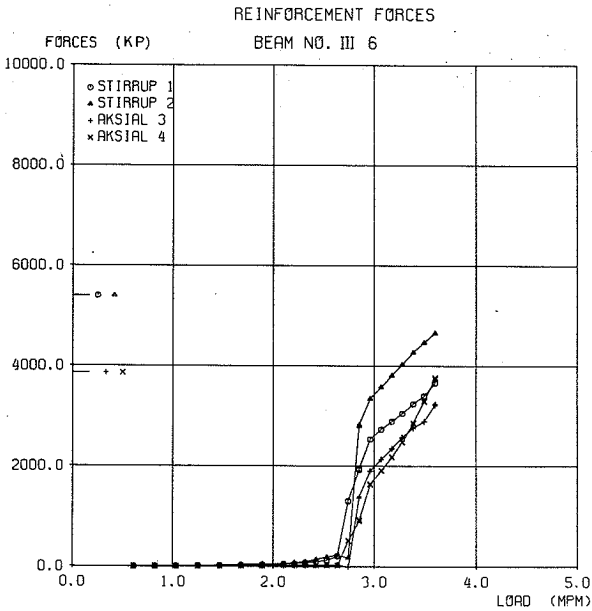
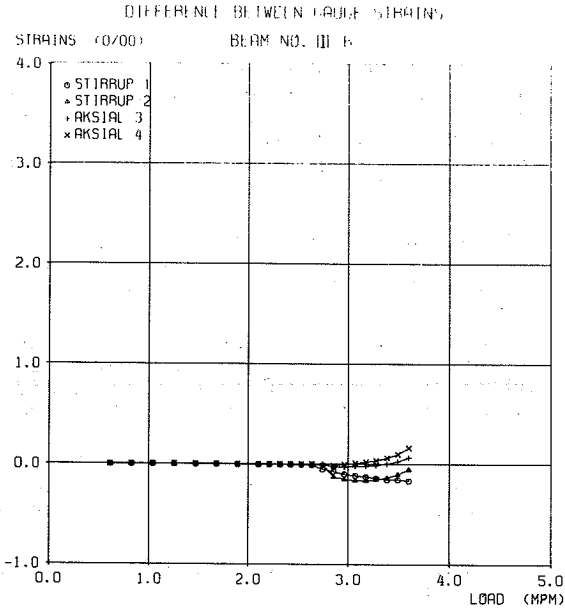


ROTATIONS

BEAM NO. III 6







REFERENCES:

- [ 1 ] Denis Mithell, Paul Lampert and Michael P. Collins: "The Effects of Stirrup Spacing and Longitudinal Restraints on the Behaviour of Reinforced Concrete Beams Subjected to Pure Torsion". Publication 71-22, October 1971. Department of Civil Engineering, University of Toronto.
  
- [ 2 ] M.P. Nielsen: "Kombineret bøjning og vridning af jernbetonbjælker". Danmarks Ingeniørakademi, Bygningsafdelingen, Aalborg. Rapport 7103, 1971.
  
- [ 3 ] J. Sander Nielsen: "A Theoretical and Experimental Study of Concrete Beams - Especially Over-Reinforced Beams - Subjected to Torsion". Ph.D. Thesis. Afdelingen for Bærende Konstruktioner, Danmarks Tekniske Højskole, 1982.
  
- [ 4 ] P. Lampert, P. Lüchinger und B. Thürlimann: "Torsionsversuche an Stahl- und Spannbetonbalken". Institut für Baustatik, ETH, Zürich. Bericht Nr. 6506-4, 1971.
  
- [ 5 ] H.J. Larsen: "Teknisk elasticitets- og styrkelære". København, 1969.
  
- [ 6 ] S. Gravesen, S. Traberg: "Relaxationsforsøg med 0,6" forspændingsliner". Sagsrapport Nr. S 18/75, 1978. Afdelingen for Bærende Konstruktioner, Danmarks Tekniske Højskole, Lyngby.

AFDELINGEN FOR BÆRENDE KONSTRUKTIONER  
DANMARKS TEKNISKE HØJSKOLE

Department of Structural Engineering  
Technical University of Denmark, DK-2800 Lyngby

SERIE R

(Tidligere: Rapporter)

- R 126. GIMSING, NIELS J.: Four Papers on Cable Supported Bridges. 1980.
- R 127. SVENSSON, SVEN EILIF og JAN KRAGERUP: Interaktiv bæreevne af sammensatte søjler. 1980.
- R 128. GIMSING, NIELS J. og JØRGEN GIMSING: Analysis of Erection Procedure for Bridges with Combined Cable Systems. Cable Net Bridge Concept. 1980.
- R 129. ROSTAM, STEEN og EIGIL STEEN PEDERSEN: Partially Prestressed Concrete Bridges. Danish Experience. 1980.
- R 130. BRØNDUM-NIELSEN, TROELS: Stress Analysis of Cracked Arbitrary Concrete Section under Service Load. 1981.
- R 131. BRINCKER, RUNE: Plane revneudvidelsesproblemer i lineært viscoelastiske materialer. Løsning af plane lineært viscoelastiske randværdiproblemer med kendt revneudbredelsesforløb. 1982.
- R 132. BRINCKER, RUNE: Plane revneudbredelsesproblemer i lineært viscoelastiske materialer. Revnemodeller og udbredelseskriterier. 1983.
- R 133. Reserveret.
- R 134. ABK's informationsdag 1981. 1981.
- R 135. Resuméoversigt 1980. Summaries of Papers 1980. 1981.
- R 136. BACH, FINN og M.P. NIELSEN: Nedreværdiløsninger for jernbetonplader. 1981.
- R 137. Publication pending.
- R 138. NIELSEN, LEIF OTTO og PETER NITTEGAARD-NIELSEN: Elementmetodeberegninger på mikrodatamat. 1981.
- R 139. MONDORF, P.E.: Concrete Bridges. Literature Index. 1981.
- R 140. NIELSEN, METTE THIEL: Lamb's Problem. Internal Harmonic Point Load in a Half-Space. 1981.
- R 141. JENSEN, JESPER FRØBERT: Plasticitetsteoretiske løsninger for skiver og bjælker af jernbeton. 1982.
- R 142. MØLLMANN, H.: Thin-Walled Elastic Beams with Finite Displacements. 1981.
- R 143. KRAGERUP, JAN: Five Notes on Plate Buckling. 1982.
- R 144. NIELSEN, LEIF OTTO: Konstitutiv modellering af friktionsdæmpning. 1982.
- R 145. NIELSEN, LEIF OTTO: Materiale med friktion til numeriske beregninger. 1982.
- R 146. Resuméoversigt 1981. Summary of Papers 1981. 1982.
- R 147. AGERSKOV, H. and J. BJØRNBAK-HANSEN: Bolted End Plate Connections in Round Bar Steel Structures. 1982.
- R 148. NIELSEN, LEIF OTTO: Svingninger med friktionsdæmpning. 1982.
- R 149. PEDERSEN, CARL: Stability Properties and Non-Linear Behaviour of Thin-Walled Elastic Beams of Open Cross-Section. Part 1: Basic Analysis. 1982.
- R 150. PEDERSEN, CARL: Stability Properties and Non-Linear Behaviour of Thin-Walled Elastic Beams of Open Cross-Section. Part 2: Numerical Examples. 1982.



- R 151. KRENCHER, HERBERT and HANS WINDBERG JENSEN: Organic Reinforcing Fibres for Cement and Concrete. 1982.
- R 152. THIEL, METTE: Dynamic Interaction between Soil and Foundation. 1982.
- R 153. THIEL, METTE: Soil-Pile Interaction in Horizontal Vibration. 1982.
- R 154. RIBERHOLT, H. og PER GOLTERMANN: Sømmede træbjælker. 1982.
- R 155. JENSEN, JENS HENNING: Forkammede armeringsstængers forankring, specielt ved vederlag. 1. del. 1982.
- R 156. JENSEN, JENS HENNING: Forkammede armeringsstængers forankring, specielt ved vederlag. 2. del. Appendix A til F. 1982.
- R 157. ARPE, ROBERT and CLAES DYRBYE: Elasto-Plastic Response to Stochastic Earthquakes. 1983.
- R 158. WALD, FRANTISEK: Non-Linear Analysis of Steel Frames (with Special Consideration of Deflection). 1983.
- R 159. BRØSTRUP, MIKAEL W.: Ten Lectures on Concrete Plasticity. Course given in Nanjing, China, October 1982. 1983.
- R 160. FEDDERSEN, BENT og M.P. NIELSEN: Opbøjet spændarmering som forskydningsarmering. 1983.
- R 161. KRAGERUP, JAN: Buckling of Rectangular Unstiffened Steel Plates in Compression. 1983.
- R 162. FEDDERSEN, BENT og M.P. NIELSEN: Revneteorier for enaksede spændingstilstande. 1983.
- R 163. Reserveret.
- R 164. GIMSING, NIELS J.: Preliminary Design and Optimization of Cable Systems for Bridges. 1983.
- R 165. Resuméoversigt 1982. Summaries of Papers 1982. 1983.
- R 166. NITTEGAARD-NIELSEN, PETER, JOHN FORBES OLESEN og HILMER RIBERHOLT: Elementmetodeberegning af skiveafstivede lamelkonstruktioner. 1983.
- R 167. RIBERHOLT, HILMER og PETER SPØER: Indlimede bolte til indfæstning af vingerne på Nibemølle-B. 1983.
- R 168. GIMSING, NIELS J. and ANDERS BORREGAARD SØRENSEN: Investigations into the Possibilities of Constructing Bridges with a Free Span of 3000 m. 1983.
- R 169. NIELSEN, LEIF OTTO: Randelementmetoden til 3-dimensional spændingsanalyse. 1983.
- R 170. NIELSEN, JOHN SANDER: A Theoretical and Experimental Study of Concrete Beams - Especially Over-Reinforced Beams - Subjected to Torsion. Part I. Theory. 1983.
- R 171. NIELSEN, JOHN SANDER: A Theoretical and Experimental Study of Concrete Beams - Especially Over-Reinforced Beams - Subjected to Torsion. Part II. Experiments. 1983.
- R 172. LANGSØ, H.E. og V. ASKEGAARD: Sammenhæng mellem frostdbrydning af jernbetonbjælker og ændring af frekvensspektrum, dæmpningsforhold og bæreevne. 1983.
- R 173 - R 176. Reserveret. Publication pending.
- R 177. AGERSKOV, H. and J. BJØRNBAK-HANSEN: Optimum Design of Corner-Supported Double-Layer Space Trusses. 1983.

Abonnement 1.7.1983 - 30.6.1984 kr. 110,-.  
 Subscription rate 1.7.1983 - 30.6.1984 D.Kr. 110,-.